Article

Monitoring Hazards in Dam Environments Using Remote Sensing Techniques: Case of Kulekhani-I Reservoir in Nepal

Bhagawat Rimal [1] **and Abhishek Tiwary** [2,*]

1   College of Applied Sciences (CAS)-Nepal, Tribhuvan University, Kathmandu 44613, Nepal;
     bhagawat.rimal@casnepal.edu.np or bhagawatrimal@gmail.com
2   School of Engineering and Sustainable Development, De Montfort University, Leicester LE1 9BH, UK
*   Correspondence: abhishek.tiwary@dmu.ac.uk

Abstract: Maintaining the operability of a hydroelectric power station at a scale originally designed is being compromised by continuous reservoir sedimentation. The underlying factors include a complex mix of landscape alterations owing to natural and anthropogenic activities around dam areas, such as gully erosion, landslides, floods triggered by heavy rainfall, climate change, and construction activities. The hydropower projects in the low-to-mid mountain regions of Nepal are witnessing a combination of these phenomena, affecting their optimal performance in meeting long-term sustainable power supply targets. This paper presents a combination of geo-spatial analysis and field evaluations to identify the trends from Kulekhani-I, one of the oldest storage-type hydropower projects in Nepal, using long-term time series remote sensing satellite imagery from 1988 to 2020. Our analysis shows an expansion of the surface water content area over time, attributed mainly to high sedimentation deposition owing to multiple factors. This study has identified an urgent need for addressing the following two key contributory factors through an effective control mechanism to avoid rapid sedimentation in the reservoirs: natural—landslides and floods leading to mainly silt deposition during heavy rainfalls; and anthropogenic—road construction materials dumped directly in the reservoir. Effective implementation of a remote sensing monitoring scheme can safeguard future damages to dam environments of more recently built storage-type hydropower projects.

Keywords: dam environment; land use land cover changes; NDWI; remote sensing; sedimentation

1. Introduction

Over the last decade, high hill and mountain hydrological processes have increasingly been influenced by the dynamics in human population growth, climate change, land use change, erosion, landslides, and sedimentation [1]. Typical land use/land cover (LULC) changes in dam environments include changes to water surface sediment deposition, surface run-off, stream flow, and water logging and recharge, each having a potentially adverse impact on the hydrological process. Multiple geomorphic activities in the Himalayan region of Nepal have been driven by landslides and monsoonal precipitation [2]. Land use change activities and sediment deposition, largely attributed to infrastructure development and landslide events, have been found to directly and/or indirectly impact the long-term performance of hydropower projects in Nepal [3,4]. To date, Nepal's open and liberal foreign investment policy has attracted multiple international players involved in short-term hydropower projects and associated infrastructure development activities [5–7]. However, the developers seldom attend to the long-term maintenance failures and subsequent environmental challenges, which are currently impacting the majority of the power plants in the high hills of Nepal by excessive sediment deposition in the dam areas. Indeed, gully erosion and land use change activities pose significant challenges to the lifespan and production capacity of hydroelectric plants in Nepal. The accumulation of sediments in reservoirs due to erosion can reduce their storage capacity, affecting the efficiency and functionality of

hydropower projects. In addition, changes in land use, such as deforestation or improper agricultural practices, can further exacerbate erosion and sedimentation issues [8,9]. It is noteworthy that such hydro-geomorphic attributes and their drivers are too complex to measure at spatial and temporal scales in such topography. Adverse land use and management practices can contribute to gully erosion, which in turn can have a direct impact on reservoirs. Improper land management, including deforestation, unsustainable agricultural practices, or inadequate soil conservation measures, can lead to increased erosion and sedimentation. The sediments that are carried by erosion can then accumulate in reservoirs, reducing their storage capacity and ultimately affecting their overall functionality. Road construction work, weak fill materials, animal grazing, and residential and commercial activities have been identified as the main drivers of gully erosion [10].

Dams are constructed lakes/reservoirs, built across rivers for the storage of large volumes of water, with typical safety measures ensuring their long lifespan. Unexpected extreme events, such as floods, landslides, and earthquakes, have been attributed to sedimentation deposition or damage to their structure [11]. The increasing level of anthropogenic factors has also been identified to further affect the lifespan of dams, post-construction [12]. Both small and large dams have been impacted due to gully erosion and landslides, causing environmental degradation in the upstream part of the basin and sedimentation deposition in the downstream part [13]. Increasing pore water pressure from changes in water levels in higher elevations often leads to more intense run-off and soil erosion [14], thereby compromising soil stability [15]. Topography, including factors such as elevation, slope, aspects, and curvature, significantly influences gully erosion by affecting water flow, soil stability, and erosion rate [14]. The trend of rainfall, landslides, geological conditions, and human activities have an influence on reservoir water levels.

Advanced remote sensing technology has already been utilized for the monitoring and management of river barriers, changing water bodies of reservoirs [16], and the extraction of specific spectral features in the spatial analysis of dam environments globally [17]. For example, the displacement landslide area was observed in the Punatsangchhu-1 dam using InSAR remote sensing data, and found that the unstable area was larger, which impacted the dam area [18]. Anthropogenic activities around the dam area of the Mureau reservoir in Kenya were found to affect its storage capacity [19]. In most cases, this is largely attributed to sediment deposition and the consequential reduction in reservoir capacity [20]. Streambank erosion, stream segments, and sediment load have been observed in many reservoirs, mainly due to the climate change impact [21]. Some studies have evaluated the climate change impact on the performance of hydropower projects in high mountain regions of Asia [22,23]. Intense precipitation clusters, associated with climate change, have been attributed to increasing dam failure risk in the USA [24]. A spatial analysis of the climate change impact on hydropower plants of varying capacities in Nepal has shown such impacts being potentially higher for larger-sized plants [22], with continuing sedimentation in the reservoirs being the prime concern [25]. The majority of dam failures and their associated fatalities have resulted from either flooding following heavy precipitation [26] or glacial lake outburst flood (GLOF) events [27], often leading to the overwhelming, and destruction, of downstream hydropower plants.

Recent approaches implementing artificial intelligence (AI) tools supporting advanced computational algorithms for the detection of environmental consequences, such as LULC changes, gully erosion, and waterlogging susceptibility have also emerged [28]. A number of studies have already utilized multiple attributes and algorithms to monitor the sedimentation deposition in dam areas [19], climate change impact [22,23,29], landslide impact using remote sensing technology [18,30], and land use/land cover change around the dam area due to anthropogenic factors [11]. It is widely acknowledged that the impacts of landslides in countries like Nepal are indeed increasing over time. This consensus is based on various factors, such as changing climate patterns, deforestation, improper land use practices, and population growth, which contribute to the vulnerability of areas prone to landslides. Various previous studies have accepted the strong spatial correlation between

road construction and landslides in the hill area [31,32]. Remote sensing technology enables the monitoring and analysis of the dynamics of natural activities through the temporal mapping of water levels, landslides, new water bodies, and the land use land cover change events area observed using remote sensing tools in the water basin.

Satellite imagery can help extract and estimate the surface water content accurately [33]. Numerous methods have already been applied for the water body extraction of surface water, such as applying the Automated Glacier Extraction Index (AGEI) [34,35]; Normalized Difference Water Index (NDWI) [36–38], Modified Difference Water Index (MNDWI) [39], Normalized Difference Pond Index (NDPI) [40]; Normalized Difference Snow Index (NDSI) [41], Water-resistant Snow Index (WSI) [42], and All Band Water Index (ABWI) [43]. The majority of researchers have used Landsat images for the extraction of the water body. Multispectral satellite images with high resolution (QuickBird, GeoEye, World View) to moderate spectral resolution (Sentinel, Landsat) satellite imagery have been extensively applied for feature extraction and change analysis [44–47]. High-resolution satellites, such as QuickBird, GeoEye, and SPOT6/7, have been used to extract detailed information on water bodies [48].

However, there is a research gap in the long-term hazard monitoring of dam environments from rapid sedimentation in reservoirs combining natural and anthropogenic impacts through spatial analysis of remote sensing data. This paper presents a framework to assess the spatio-temporal dynamics in the hazard monitoring of dam environments for storage-type hydropower projects, combining geo-spatial data analysis and field-level verification. This study focuses on analyzing water level extraction patterns with land use land cover change (LULC), attributed mainly to infrastructure development and landslide events, using long-term high-resolution satellite imagery, augmented by field validation using local-level experiences of sedimentation deposition. The framework is implemented to identify the trends from Kulekhani-I, one of the oldest storage-type hydropower projects in Nepal, utilizing long-term time series remote sensing satellite imagery from 1988 to 2020 (i.e., Landsat images, Quick Bird, GeoEye, SPOT6/7). The reservoir at this site is facing several challenges, including sedimentation due to landslides, water scarcity, land use and land cover change, and a loss in its production capacity. Sedimentation refers to the accumulation of sediments in the reservoir, which can reduce its storage capacity and affect its efficiency. Water scarcity is another challenge, indicating a shortage of water supply for various purposes. Additionally, changes in land use and land cover can impact the reservoir's ecosystem and water availability. These challenges collectively contribute to a loss in the production capacity of the Kulekhani-I hydropower project's reservoir. Through long-term spatial data analysis using satellite imagery, this study has elucidated some of the underlying factors for rapid reservoir sedimentation involving a complex mix of landscape alterations and climate change owing to natural and anthropogenic activities around dam areas. The study scope includes events such as gully erosion, landslides, floods triggered by heavy rainfall, climate change, and construction activities. The analysis approach can be further developed to explore its implementation for safeguarding future damages to dam environments of more recently built storage-type hydropower projects, e.g., the Budhagandaki hydroelectricity project (BGHP) in Nepal and elsewhere globally.

2. Methodology

2.1. Study Area

The major study site is located within 85°6'7″ E to 85°11'8″ E and 27°34'20″ N to 27°39'9″ N latitude of the Kulekhani basin (Figure 1). The Kulekhani-I plant, with an installed capacity of 60 MW, was commissioned in May 1982. The dimensions of the Kulekhani dam are 7 km long and 114 m high, allowing a total "designed storage capacity" of 85.3 million cubic meters (MCMs). Of this capacity, 12 MCMs are allocated to dead storage and the remaining 73.3 MCMs to live storage [8]. Reportedly, the capacity of the Kulekhani reservoir has rapidly decreased and the surface of the reservoir has risen by

about 13 m in the last three decades [49]. Previous studies have attributed this to climate change impacts [23,50], sediment accumulation [51], etc.
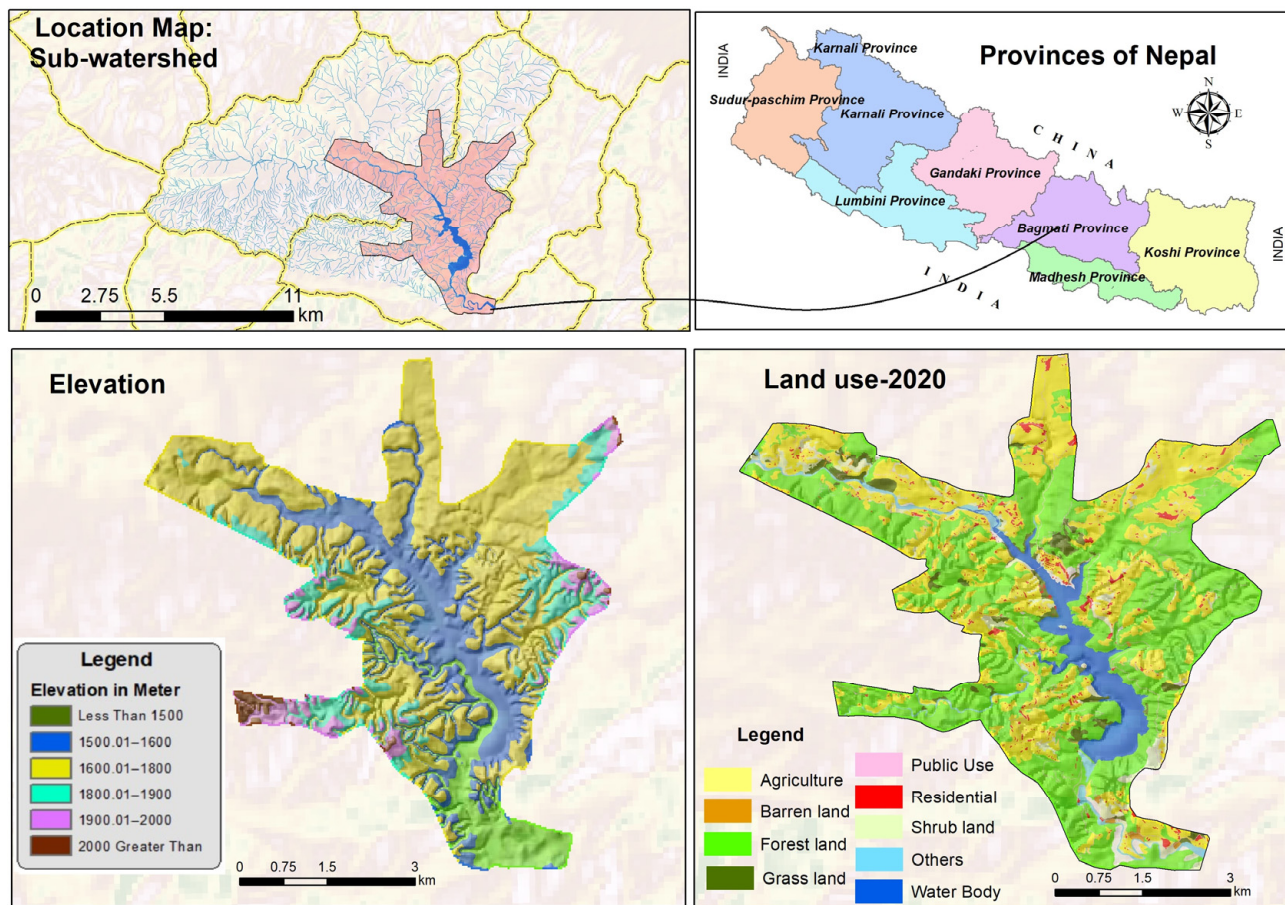

Figure 1. Study area.

2.2. Data Collection and Analysis

In this study, the remote sensing technique has been combined with extensive ground validation from field observation and verification using local information. Time series data sets from the following four satellites were used in this study—Landsat, QuickBird, GeoEye, and SPOT. Available post-monsoon season satellite images from 1988 to 2020, with maximum cloud-free 30 m resolution Landsat images (Landsat 5 Thematic Mapper, TM; Landsat 7 Enhanced Thematic Mapper Plus, ETM+; Landsat 8 Operational Land Imager, OLI), were collected from the United States Geological Survey, https://earthexplorer.usgs.gov (accessed on 27 July 2024), for the extraction of water levels of the dam area of the Kulekhani hydropower project (Table 1). All the Landsat images were registered and their accuracy was verified considering <0.5 pixel RMS errors. All images were projected in UTM Zone 45° N, Shuttle Rader Topography Mission (SRTM) Digital Elevation Model (DEM) data. The digital number (DN) of Landsat Level 1 data values of all the images were converted into radiance. The FLAASHs (Flash Line-of-sight Atmospheric Analysis of Spectral Hypercubes) atmospheric correction model was applied for radiance-corrected satellite images. Images were processed in ENVI version 5.3 and mapping was prepared in GIS.

Similarly, QuickBird imagery for 2004, GeoEye imagery for 2010, and SPOT imagery from 2012 to 2020 were acquired from https://www.l3harris.com (accessed on 27 July 2024). These high-resolution satellite images were resampled at 1.5 m resolution for constant analysis (Table 2). We used high-resolution satellite imagery for the extraction of major land use land cover (LULC) classes of the basin area and explored nine major land cover classes in the Kulekhani dam area from 2004 to 2020. Each image was further processed and classified for the long-term land use/land cover data of the study area.

Table 1. Data categories and sources.

Data Category	Source	Outputs (Reference Output Figure Numbers in Brackets)
High-resolution satellite images from 2004 to 2020	QuickBird image for the year 2004, GeoEye images for the year 2010, and SPOT for 2012–2020. https://www.l3harris.com (accessed on 27 July 2024)	Land cover classification/extraction of landslides and water body of Kulekhani 1 area (Figures 2, 5, and 10–12).
Landsat images from 1988 to 2020	Source link: https://earthexplorer.usgs.gov (accessed on 27 July 2024)	For the analysis of long-term water level extraction using NDWI method in Kulekhani reservoir and evaluation using NDVI (Figures 6–8).
Station-based precipitation and temperature data, 1985–2020	Environmental statistic, 2008, 2013, and 2019, Nepal and Department of Hydrology and Metrology, 2020.	For the analysis of long-term precipitation and temperature data (Figure 9).
Shuttle Rader Topography Mission (SRTM) Digital Elevation Model (DEM) data	Source link: https://earthexplorer.usgs.gov/ (accessed on 27 July 2024)	SRTM DEM data for the analysis of elevation, slope, and aspect (Appendix B).
Soil and Terrain (SOTER) database for Nepal	SRIC Report 2009/01: Soil and Terrain database for Nepal https://www.isric.org/documents/document-type/isric-report-200901-soil-and-terrain-database-nepal-11-million (accessed on 27 July 2024)	Soil and Terrain (SOTER) attribute data for the analysis of landslides (Appendix B).
Geology data	ICIMOD, https://rds.icimod.org/Home/DataDetail?metadataId=2521 (accessed on 27 July 2024)	Geology attribute data for the analysis of landslides (Appendix B).
Seismic hazard data level	Pandey et al., 2002 [52], GoN, 1996, [53]	Seismic hazard data for the analysis of landslides (Appendix B).

Time series Landsat 5, 7, and 8 imagery applied (Path/Row 141/041).

Year	1988	1990	1992	1994	1996	1998	2000	2002	2004	2006	2008	2010	2014	2016	2018	2020
Months	29-Nov	4-Feb	23-Oct	13-Oct	18-Oct	8-Oct	22-Nov	27-Oct	9-Nov	30-Oct	20-Nov	25-Oct	23-Dec	25-Oct	31-Oct	22-Jan
Sensor	TM	TM	TM	TM	TM	TM	ETM+	ETM+	TM	TM	TM	TM	OLI	OLI	OLI	OLI

Table 2. Source list of high-resolution time series satellite imagery applied in this study.

QuickBird (Resample 1.5 m)	01 and 03-Dec 2004
World View 2 (Resample 1.5 m)	26-Jan-2010
SPOT 1.5 m	29-Oct-2012
SPOT 1.5 m	13-Jan-2015
SPOT 1.5 m	06-Nov-2016
SPOT 1.5 m	17-Jan 2017
SPOT 1.5 m	04-Nov-2018
SPOT 1.5 m	20-Dec-2019
SPOT 1.5 m	01-Nov-2020

The applied image analysis methods were as follows: Artificial Neural Network (ANN) [54], Convolutional Neural Networks (CNNs), K-Nearest Neighbor (K-NN) model [55], kernel-based textural granulometry method [46], Logistic Model (LM) [56], Maximum Likelihood (ML) classifier, and Random Forest (RF) classifier [57]. The Support Vector Machine (SVM) machine learning technique was applied for the extraction of land cover classes of the study area following the literature [58,59]. SVM algorithms are a flexible supervised classifier option with higher accuracy [60–65].

$$\text{Linear}: K\,(xi,\,yi)\ =x_i^T\cdot x_j,$$

$$\text{Polynomial}: K\,(xi,\,yi)\ =(g\cdot x_i^T\cdot x_j+r)^d,\,g>0,$$

$$\text{Radial basis function}: K\,(xi,\,yi)\ =\mathrm{e}^{-g(x_i-x_j)^2},\,g>0,$$

$$\text{Sigmoid}: K\,(xi,\,yi)\ =\tanh\,(g\cdot x_i^T\cdot x_j+r)$$

where, g, d, and r are user-controlled parameters of the kernel function.

The classified raster data were converted into vector format and very small silver polygons were corrected in GIS. We identified nine major land cover types across a 29 sq. km area of the Kulekhani basin of the study area (Table 3 and Figure 2), with 93% overall accuracy. Among the barren lands, we noticed major landslides and other land use changes in close vicinity of the reservoir using GPS and collected satellite images.

Table 3. Land use/cover classification schemes.

| Land Cover Types	Description
Cultivated land	Orchards, wet and dry crop lands
Forest	Evergreen broad leaf forest, deciduous forest, temperate forest, low density sparse forest, degraded forest, mix of trees, and other natural covers
Grass	Mainly grass fields (dense coverage grass, moderate coverage grass, and low coverage grass)
Shrub	Mix of short trees, other natural covers, and highly degraded forest
Water	Reservoir, river, lake/pond, canal, and swamp areas
Other land	Sandy areas, river banks, other areas
Barren land	Cliffs/landslides, bare rocks, other unused land
Public use	Road network, and other construction features
Residential	Residential area (urban and rural settlements), commercial areas, industrial
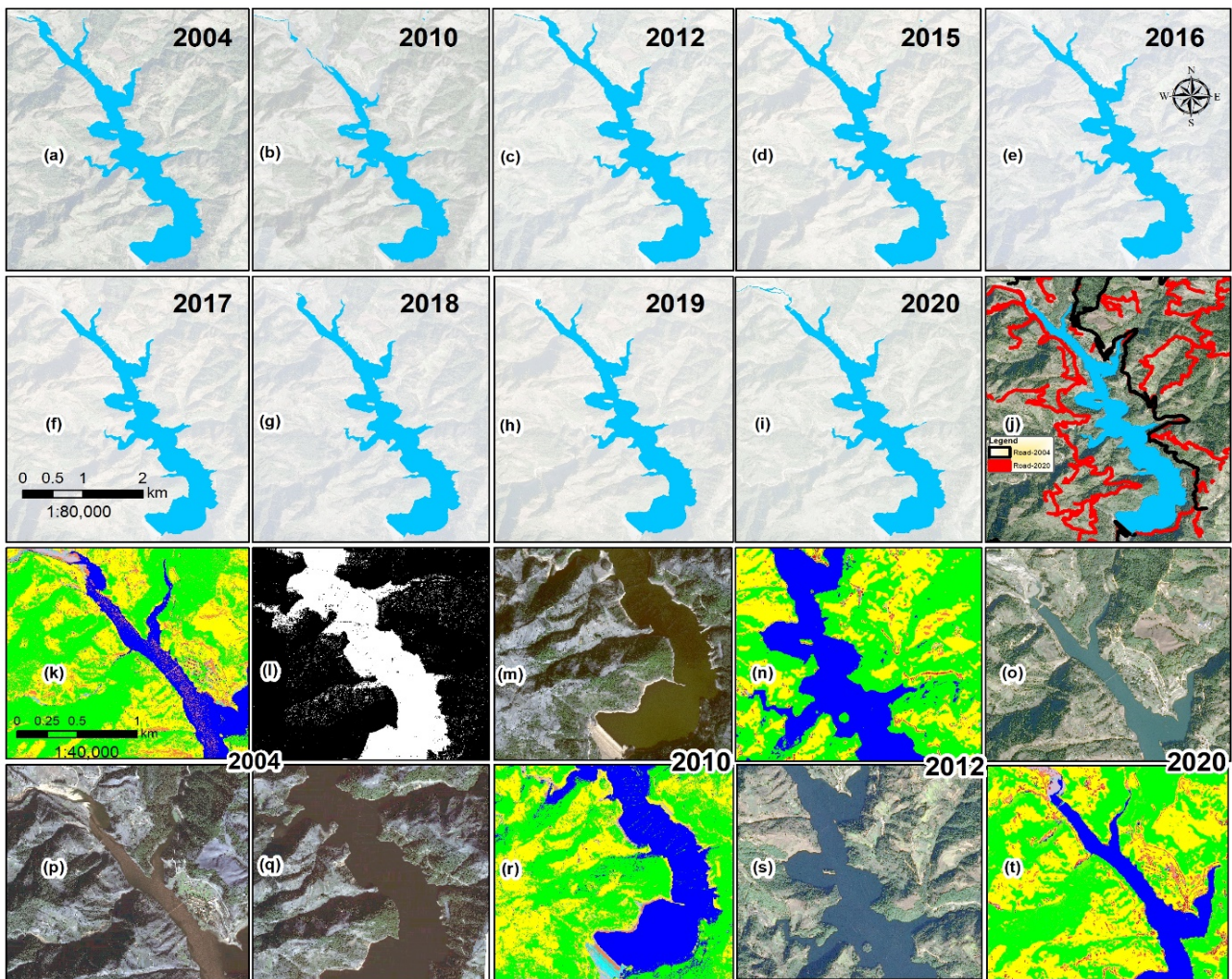
Figure 2. (**a–i**) Surface water of reservoir; (**j**) road network in 2004 and 2020; (**k–t**) satellite images and classification using SVM approach in 2004, 2010, 2012, and 2020.

2.3. Spatial Analysis Description

We evaluated surface water content reduction/expansion in the dam area between 1988 and 2020, applying the Normalized Difference Water Index (NDWI) from Landsat satellite images [34,38,66,67]. The positive NDWI threshold value of 0 to 1 was acceptable for the evaluation [24,68], and the extraction NDWI equations were applied [36] (Equations (1) and (2)).

$$NDWI^{OLI} = \frac{Green\ (Band\ 3) - NIR\ (Band\ 5)}{Green\ (Band\ 3) + NIR\ (Band\ 5)} \tag{1}$$

$$NDWI^{TM}\ and\ NDWI^{ETM+} = \frac{Green\ (Band\ 2) - NIR\ (Band\ 4)}{Green\ (Band\ 2) + NIR\ (Band\ 4)} \tag{2}$$

Furthermore, the Normalized Difference Vegetation Index (NDVI) value has been evaluated to understand the forest area change within the study boundary. The normalized value has been evaluated between −1.0 and +1.0, with full vegetation coverage defined by Equations (3) and (4):

$$NDVI^{OLI} = \frac{NIR(Band\ 5) - Red(Band\ 4)}{NIR(Band\ 3) + Red(Band\ 5)} \tag{3}$$

$$NDVI \; and \; NDVI^{ETM^+} = \frac{NIR(Band \; 4) - Red(Band \; 3)}{NIR(Band \; 4) + Red(Band \; 3)} \tag{4}$$

2.4. Evaluation of Major Landslide and Preparation of Landslide Risk Map

Landslides are among the most dangerous geological hazards in terms of damaging infrastructure and environmental balances and are strongly influenced by geology, slope, precipitation, land cover changes, and population activities [69–73]. Both triggering and causing factors play major roles in landslide occurrences [74]. Despite the severe consequences of landslides, there is a noticeable deficiency in their susceptibility assessments and risk management strategies to date [71]. To acquire an overview of the pressure of landslides in the reservoir area under study, landslide sample data were collected using the global positioning system during fieldwork. Furthermore, the existing landslide trends were collected from Google Earth imagery, QuickBird, GeoEye, and SPOT6/7. Historical landslide events were redrawn by the manual identification of landslide features during the land use/cover data preparation time using time series images (Table 2). Field verification was conducted for the validation and preparation of the landslide risk map (Figure 3). The inventory included shallow, soil landslides, and deep bedrock landslides. We captured the landslide area where landslides generally occurred and excluded the low land around/inside of the dam. For the analysis of landslide hazards, Shuttle Rader Topography Mission (SRTM) Digital Elevation Model (DEM) data were used for terrain analysis, including slope and aspect layers. The existing triggering factors, precipitation levels, scenic hazard and susceptibility/causing factors (slope, aspect), geology/lithology, drainage density, relative relief, land use/cover, Soil and Terrain (SOTER) database, as well as knowledge-based analysis were used for the evaluation of the landslide hazard map and risk zone of the study area (Appendices A and B). The landslide susceptibility/risk mapping was classified into high, moderate, low risk, and no risk (i.e., stable zones) in terms of landslide hazards in the study area. This approach followed the evaluation of landslide risk in previous research [74].

The identification and assessment of the landslide factors were conducted using remote sensing, hydrological, and statistical techniques, considering the highest landslide prediction rate for the highest overall weighting [75]. Similarly, the station-based temperature and rainfall data were collected for further analysis of climate change impacts in the study area from the Department of Hydrology and Meteorology (DHM), Nepal. The framework for mapping and modeling applied in this study is schematically presented in Figure 4. Further, the applied landslide risk mapping framework is presented in Appendix A.

(a)   (b)

Figure 3. Collection of field level information: (**a**) reading of satellite images, and (**b**) field verification.
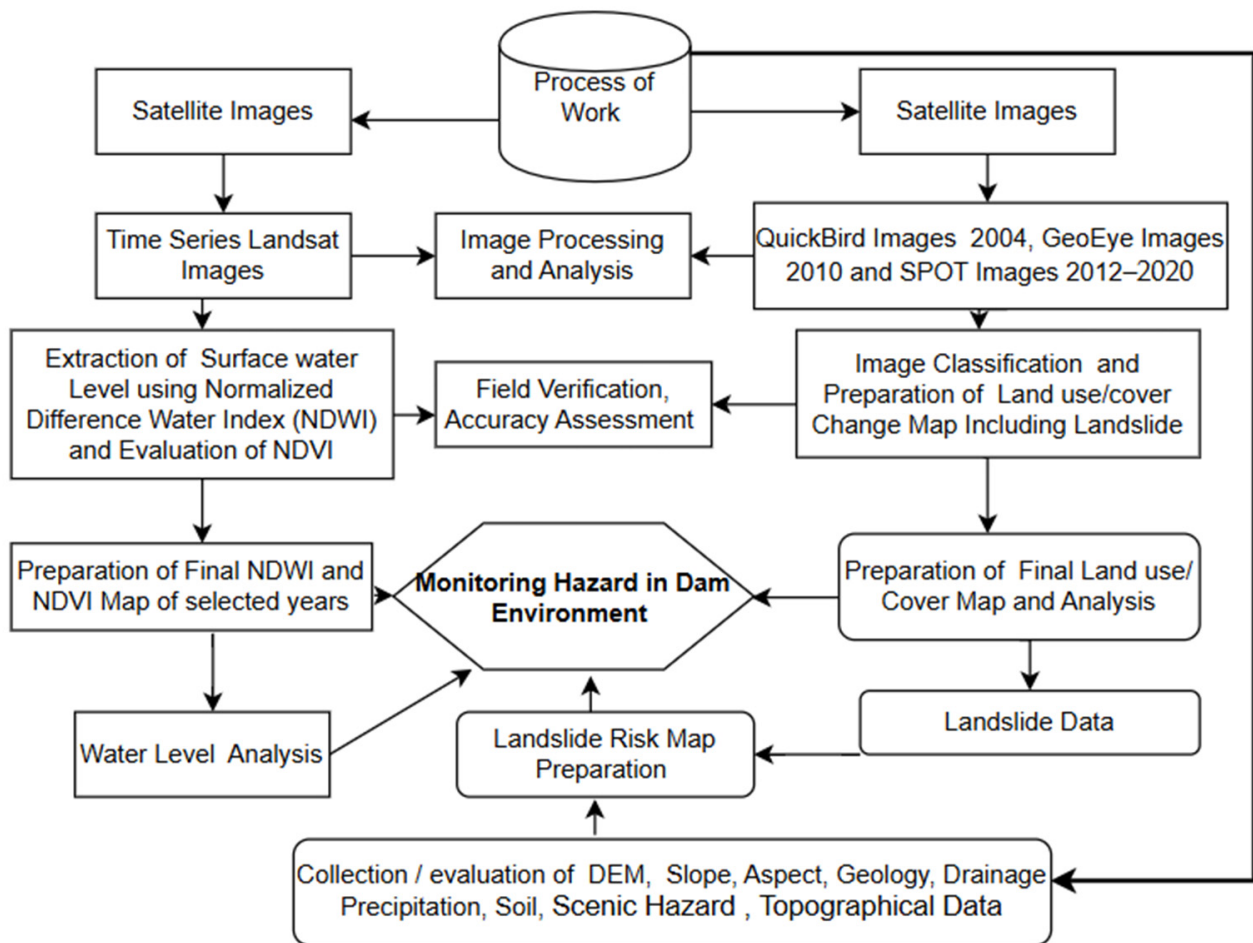
Figure 4. Mapping and modeling framework.

3. Results

3.1. Land Use Land Cover Change and Its Impact on the Dam Environment

According to the analysis, there is a remarkable change in LULC in the Kulekhani basin in the vicinity of the dam area—the residential area increased from 25.19 ha (hectares) to 55.49 ha between 2004 and 2020. Similarly, use of public land increased from 17.38 ha to 50.74 ha, grassland increased from 69.25 ha to 84.66 ha, forest land increased from 1264.89 ha to 1412.75 ha, and barren land increased from 22.12 ha to 32.36 ha. However, there is an indication that over the same period, the water body, shrubland, agricultural, and other land categories decreased (Table 4, Figure 5). Both image analysis results and field observations indicate the following: infrastructure (road network) development activities have shown an increasing trend, represented by the increase in public land. Urban development processes such as new building construction for residential/institutional/industrial purposes have rapidly replaced agricultural land. However, water resource management practice near the dam area is observed to be poor and largely overlooked. Specifically, there are no control mechanisms in place to avoid landslides and landslips, which are found in the close vicinity of the dam area. Further, a recent infrastructure development push by the provincial and local governments has encouraged the development of road connectivity, with an increasing number of road buildings, contributing to rubble being left along the roadside, which often gets swept away during the monsoon season. A spatial analysis shows an increase in barren land in the Kulekhani area (Table 4), largely attributed to the increasing number of landslides around the dam area, subsequently leading to increased sedimentation deposition in the reservoir.
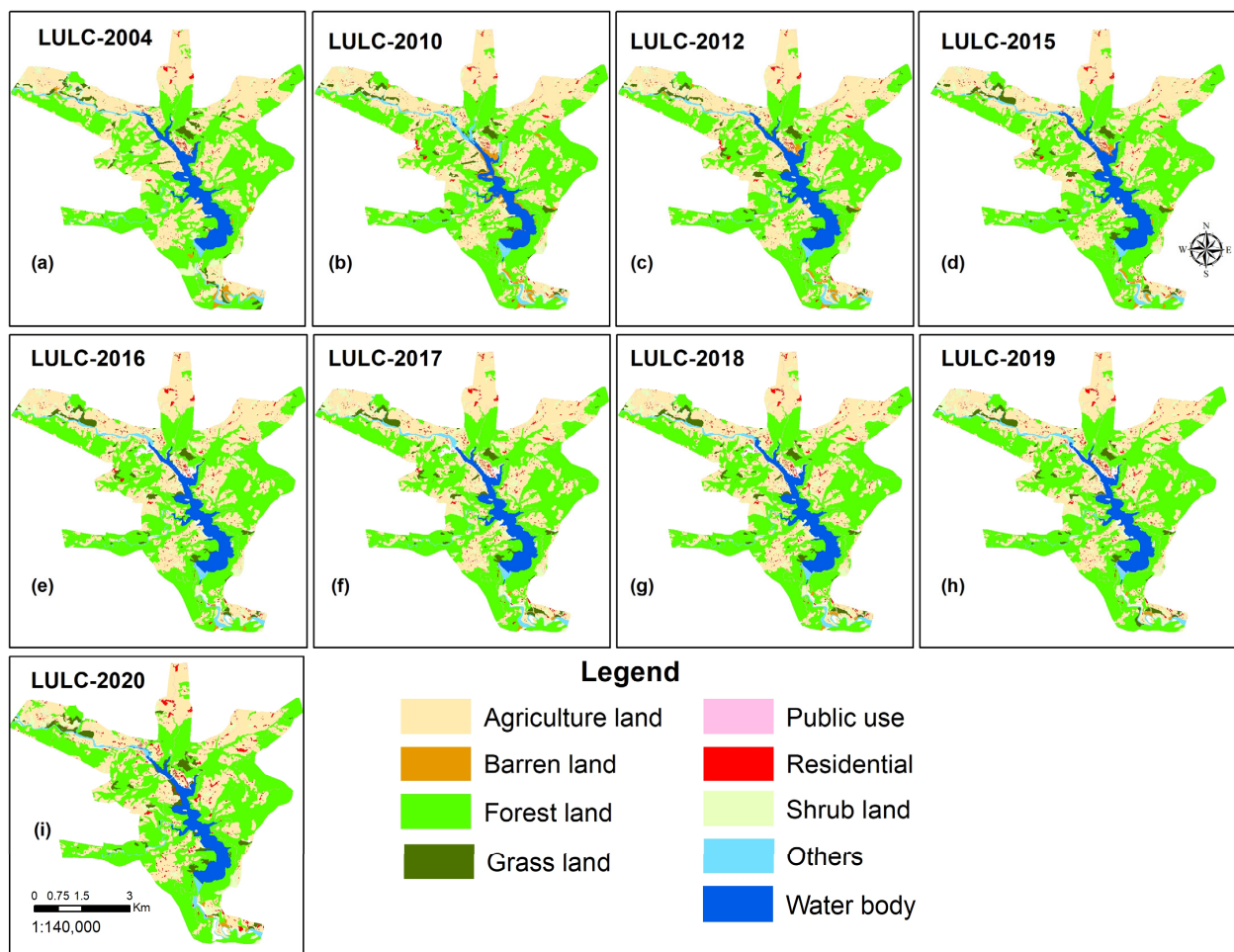
Figure 5. Land use land cover maps for the study site from 2004 to 2020: (**a**) 2004; (**b**) 2010; (**c**) 2012; (**d**) 2015; (**e**) 2016; (**f**) 2017; (**g**) 2018; (**h**) 2019; and (**i**) 2020.

The evaluation of the surface water level of the dam area is estimated using NDWI mean values from 1988 to 2020. Our analysis shows that the surface water level of the Kulekhani dam has increased, represented by an increase in NDWI values from 0.182 in 1988 to 0.405 in 2020 (Figures 6 and 7). In the early part (1990–1994), the NDWI value remained low; however, it increased rapidly beyond 1994, indicating a larger part of the submerged area due to the dam. This could be attributed to multiple factors, such as climate change impact, variance of precipitation, landslides, earthquakes, and sediment deposition. It seems that the level of surface water is not constant in the reservoir area. The forest cover area is an increasing trend, and the NDVI value showed the green part of the watershed area is higher than in previous years (Figure 8).
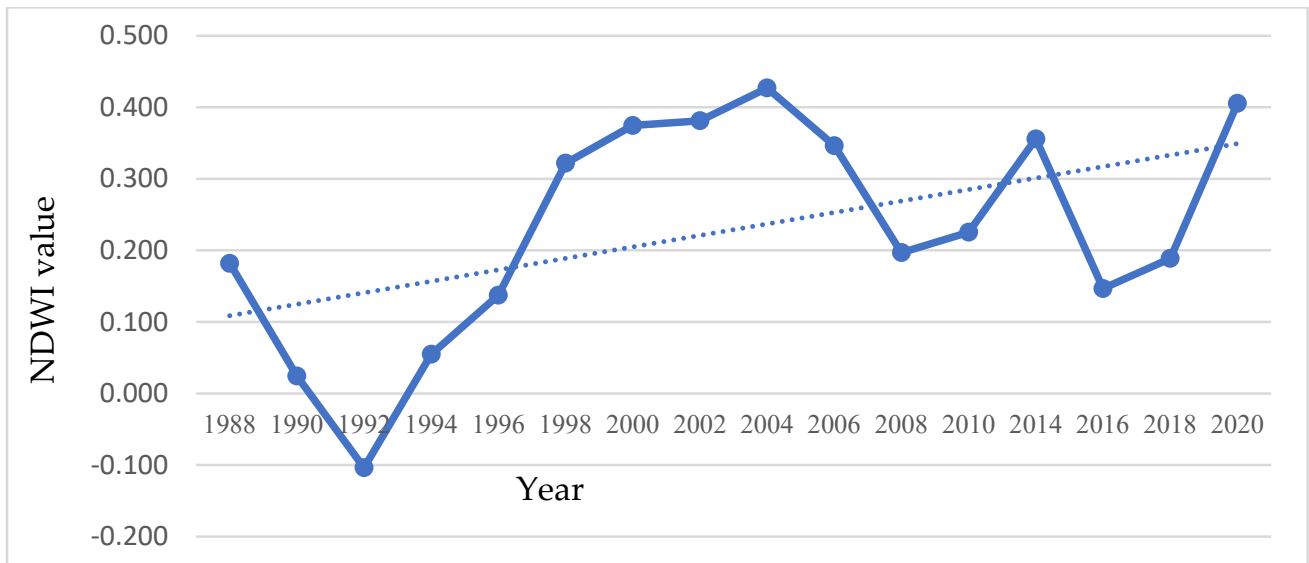
Figure 6. Time series graph for the NDWI mean pixel values from 1988 to 2020.
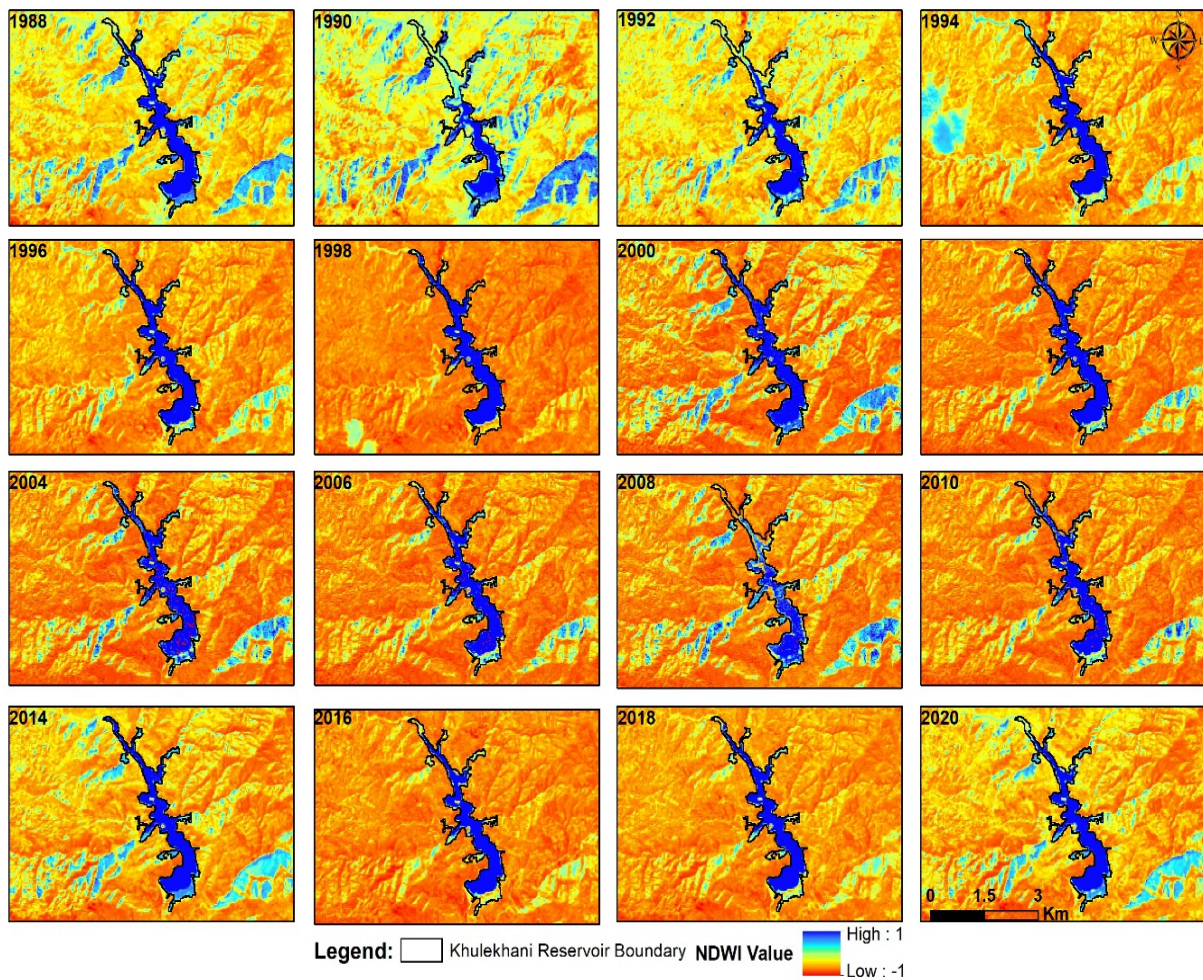

Figure 7. NDWI scene maps (Landsat images) of the dam area between 1988 and 2020.
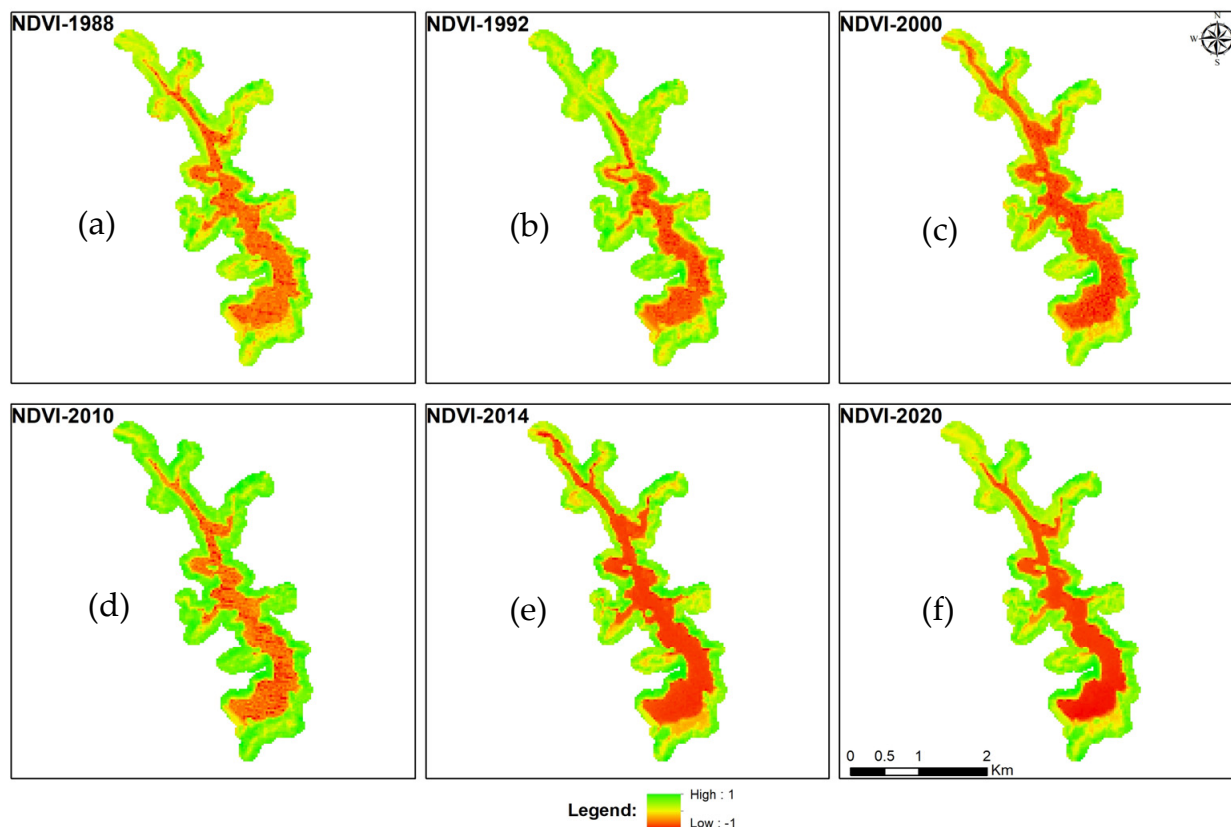
Figure 8. NDVI of Kulekhani dam area. (**a**) NDVI, 1988; (**b**) NDVI, 1992; (**c**) NDVI, 2000; (**d**) NDVI, 2010; (**e**) NDVI, 2014; (**f**) NDVI, 2020.

Table 4. Land cover change analysis results (area in hectares).

Land Cover	2004	2010	2012	2015	2016	2017	2018	2019	2020
Agriculture	1147.94	1102.23	1083.57	1058.37	1024.39	1002.26	981.10	948.95	934.55
Forest	1264.89	1320.86	1317.44	1320.46	1331.89	1343.09	1340.86	1377.08	1412.75
Grass Land	69.25	64.85	61.09	74.20	68.60	70.51	69.65	72.00	84.66
Shrub	110.97	94.44	106.15	116.31	128.91	139.93	147.47	157.45	105.51
Water Body	194.57	140.40	195.04	196.48	180.34	177.21	188.67	172.03	181.43
Others	59.10	75.01	53.95	52.49	58.89	58.85	55.21	53.34	53.96
Barren	22.12	47.66	26.19	23.24	38.50	38.13	35.75	36.82	32.36
Public Use	17.38	31.73	31.81	31.85	38.97	38.93	46.88	47.09	50.74
Residential	25.19	34.27	36.22	38.06	40.93	42.49	45.83	46.65	55.49

3.2. Climate Change Analysis

Based on the result of the temperature and precipitation pattern analysis from the Kulekhani basin, an increasing trend of temperature and reduction in precipitation from 1985 to 2020 is noted. The temperature analysis of the Daman meteorological station (station number 905 near the Kulekhani reservoir) from 1985 to 2020 showed that the maximum mean temperature was recorded in 2009 and the minimum mean temperature was recorded in 2019. Over the same period, the annual mean temperature was observed to be increasing (Figure 9).

The annual rainfall from 1985 to 2020 is also presented in Figure 9 (right *y*-axis, in mm). While the patterns show local peaks and troughs, no clear long-term trend could be found in the annual rainfall during the study period. However, previous studies have indicated a strong spatial correlation between landslides and climate change in Nepal. These studies have highlighted the influence of climate-related factors, such as increased

rainfall intensity, changing precipitation patterns, and temperature variations, on the occurrence and frequency of landslides in various regions of western Nepal [76].
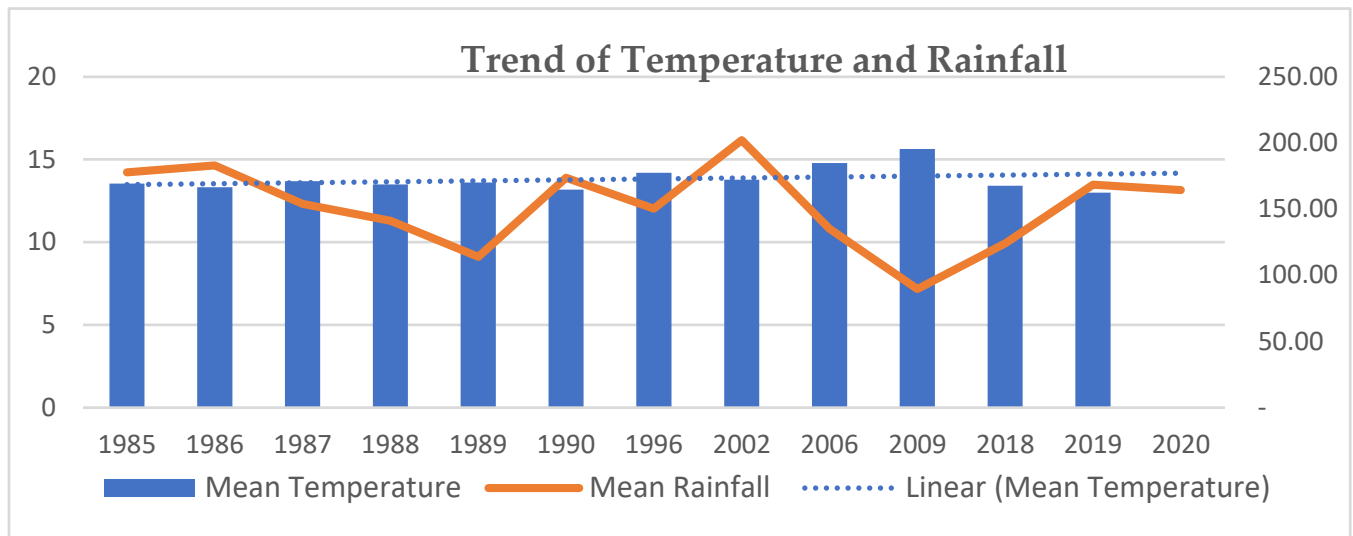

Figure 9. Annual mean temperature (left *y*-axis, deg C) and precipitation (right *y*-axis, mm) at the Daman meteorological station (close to the reservoir).

3.3. Landslide Risk Analysis

The road density in the study area is found to have increased from 0.85 to 3.13 km between 2004 and 2020 (Figure 10). The increased focus on road construction in the hill regions of rural Nepal after 2006, and the subsequent infrastructure expansion processes, have led to a higher incidence of landslides in the lower part of the Kulekhani dam site, compared to the upper part. The occurrence of these landslides is particularly observed in areas where road construction activities are taking place. The local-level reconstruction efforts in 2017 prioritized road construction, which has further contributed to the increase in landslides. It is important to note that road construction activities, particularly in hilly regions, can have a significant impact on the stability of the surrounding slopes, thereby increasing the risk of landslides. Population growth and poor land use planning can further contribute to the vulnerability level [72]. A similar trend has been reported in other parts of the hill region of Nepal [31,32].

Based on the analysis of landslide events, around a 9 ha area covered by 21 small-to-large scale dams was affected by landslides in 2004, with the majority occurring away from roads in and around the forest and dam sites. The high precipitation also supports the increase in landslides in the study area. However, in the later period, most of the landslide events occurred in roadside areas. Figure 11 provides the severity rate associated with each landslide occurrence (left *y*-axis) along with the number of landslide occurrences for that year (right *y*-axis). The severity rate represents the severity or intensity of the landslides. It was found that while 21 landslide events were observed in 2004, this increased to 38 events in 2020. Major landslide areas were spotted to occur around the dam, which has been identified to be further increasing due to a combination of natural and anthropogenic factors. Our analysis also shows that in 2020, the frequency of new landslides is higher within a 200 m range from an existing landslide area, typically where the elevation is not constant. This is mainly attributable to factors such as an over-steep slope on the uphill side of the road, the deposition of excavated debris on the downhill side, and/or the impact of heavy rainfall events and run-off from the road on the mobilization of debris.

Based on the available data, field observation, and further knowledge-based analysis, 10.22% of the study area was estimated as a stable area. The latter is considered as the area covering the reservoir water body, with no landslide risk. Similarly, a 23.67% area was estimated as a low landslide risk zone, with low slope elevation (<20 degrees), whereas 23.23% was identified as a moderate risk zone area, and a 42% area as a high-risk zone for landslide hazards (Figure 12). It is noteworthy that the elevation factor did not always determine the landslide events in the higher part of the upper stream of the study area as we observed other anthropogenic factors (like road construction activities) play a vital role in causing landslides in the study area.

Based on the remote sensing data analysis, field observation, and local-level information gathering, it has been determined that the accumulation of sediments in the reservoir poses a significant challenge, mainly affecting the storage capacity of the reservoir. Over time, sediments gradually settle at the bottom of the reservoir, reducing the available space for water storage. As a result, the water level in the reservoir rises, overwhelming the dam capacity and potentially leading to flash flooding events when the barriers are opened to release excess water that it cannot hold. Managing sedimentation involves implementing various techniques and practices to control and minimize sediment deposition. These may include sediment trapping structures, such as sediment basins or settling ponds, which help capture and retain sediments before they reach the reservoir. In addition, sediment dredging or removal operations can be conducted periodically to restore the reservoir's storage capacity.
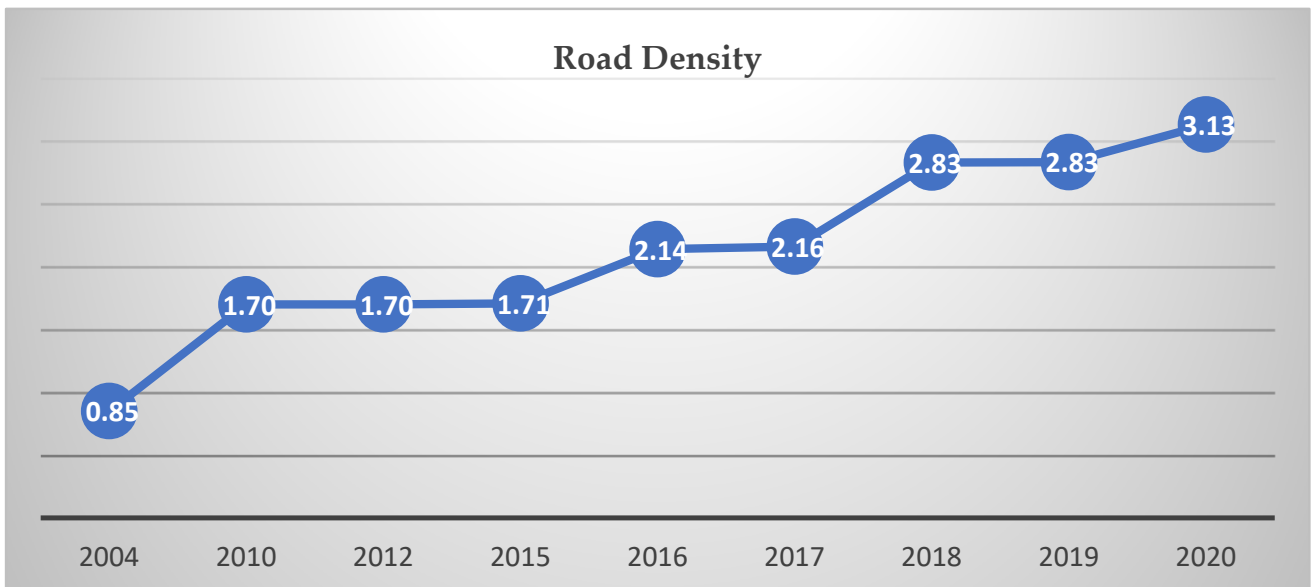

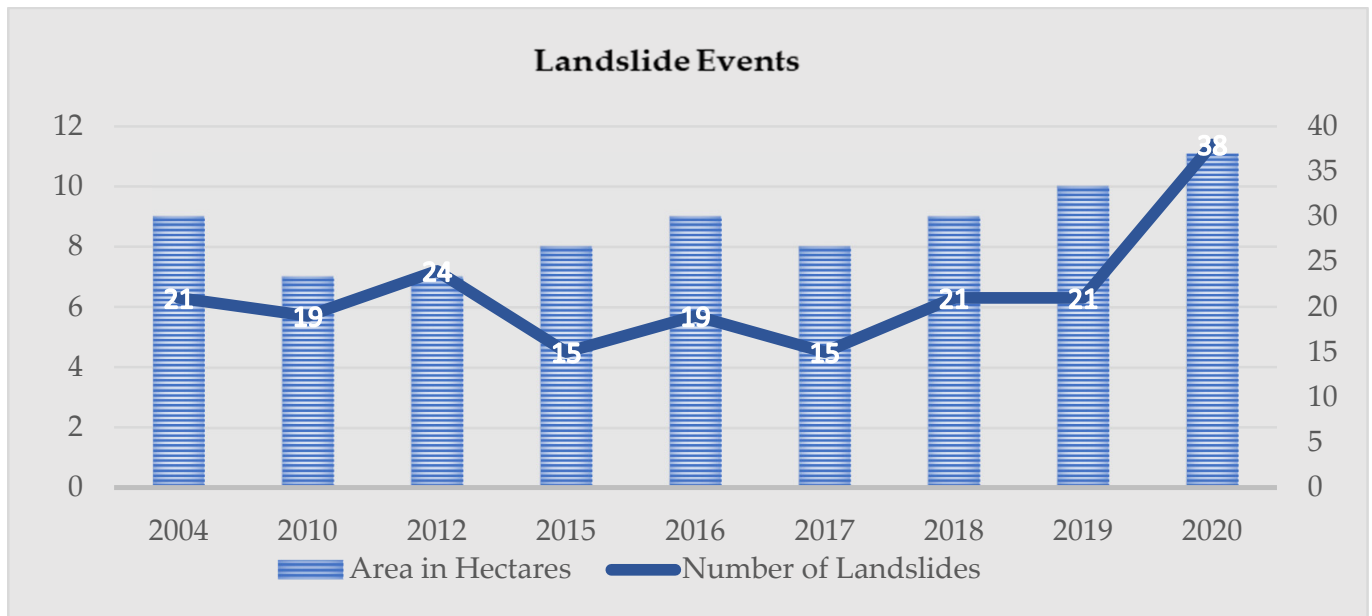**Figure 10.** Road density in the study area between 2004 and 2020.

Figure 11. Landslide events in the study area from 2004 to 2020, showing the severity rate associated with each landslide occurrence (left *y*-axis) and the number of landslide incidents (right *y*-axis).
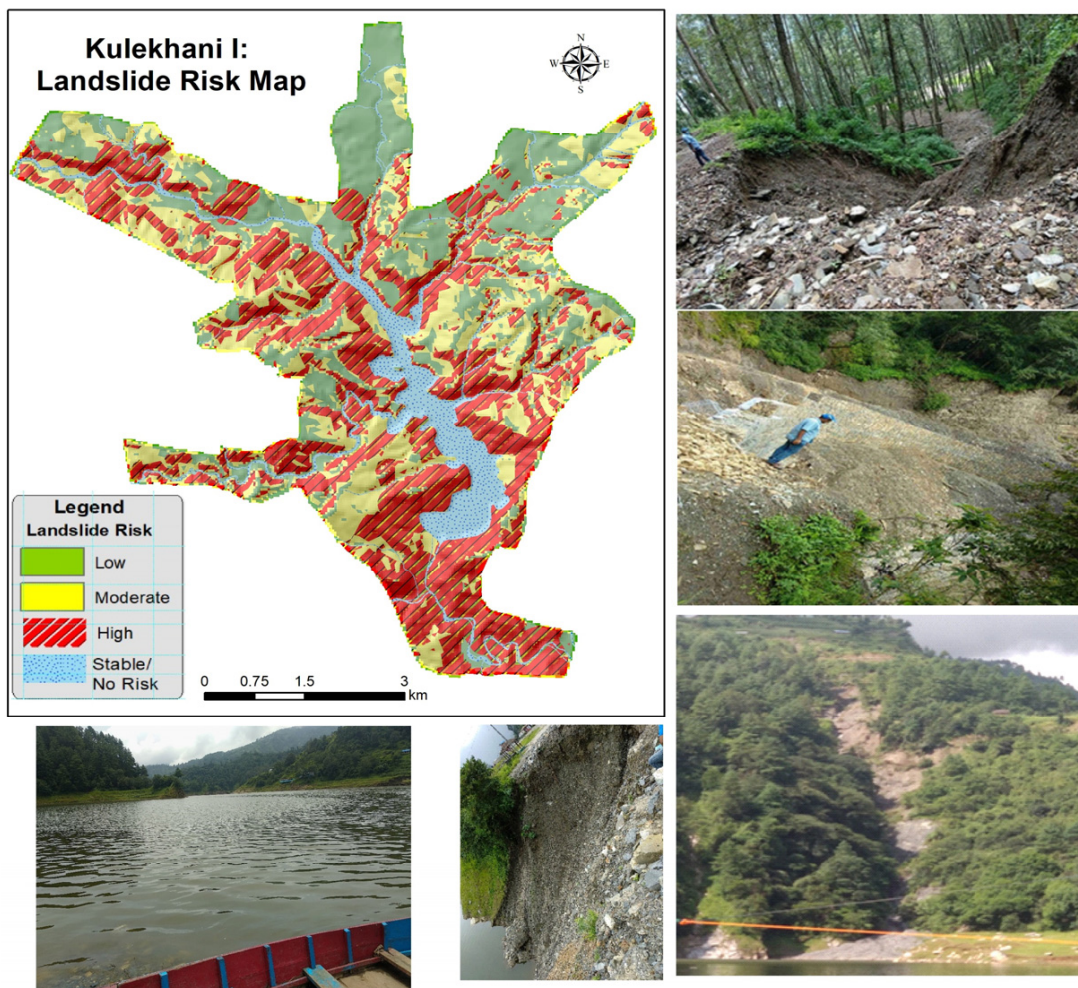

Figure 12. Landslide risk map and photo source of sediment collection in dam area due to landslide.

4. Discussion

This study primarily focused on the role of sedimentation in affecting reservoir capacity. Overall, the sedimentation status of Kulekhani is showing an increasing trend, and the discharge of the river is showing a decreasing trend. Our analysis found the following land use changes in the reservoir area from 2004 to 2020: road density increased from 0.85 km to 3.13 km; and the settlement area increased from 25.19 ha to 55.49 ha. Sedimentation deposition is particularly high around the dam area where frequent, small-scale landslides have occurred, largely associated with topography and road construction activities. The surface water level in Kulekhani dam has drastically increased between 1988 and 2020, represented by the NDWI analysis using Landsat images of 0.182 and 0.405, respectively. A local site observation inferred that there is no adequate control mechanism in place to avoid the direct release and deposition of the materials released during road construction in the reservoir, typically during monsoon (high rain) incidents. A small stream area check dam can potentially protect such types of deposition in the reservoir.

Natural events affecting the reservoir capacity over the study period include sedimentation collection and deposition during flood events and gully erosion. Such events are aggravated due to the climate change impact on long dry seasons, irregular rains, and high-intensity rainfall resulting in increased run-off and reduced infiltration. As a result, rural communities in these areas are experiencing the effects of climate change on their water resources. Specifically, increased landslides are associated with slope stability, soil moisture content, and erosion rates, thereby increasing the susceptibility of certain areas to landslides [76]. The annual mean temperature was found to have an increasing trend from 1985 to 2020; the annual mean rainfall was largely unchanged over this period. Reportedly, the capacity of the Kulekhani reservoir has rapidly decreased from 85 MCM to 60 MCM in the past decade and the surface of the reservoir has risen by about 13 m in the last three decades [49]. This has a direct impact on the power generation capacity of the Kulekhani reservoir [8], which highlights the importance of monitoring and managing sedimentation in order to maintain the functionality and efficiency of the reservoir. This is in addition to previous studies reporting the role of the climate change impact [23,50], the reduction in the precipitation ratio in monsoon time [50,77] compared to the previous decade, and the role of LULC change and its impacts in another river basin [78].

Recent trends have been alarming—heavy rainfall on 28 September 2024 led to Kulekhani reservoir gates being opened when the water level increased to the danger point [79]. The absence of disaster preparedness is leading to significant damage to hydropower projects in Nepal [80,81]. Heavy floods and landslides have already affected hydropower projects in eastern Nepal, and at least 11 hydropower projects with a total capacity of 107.54 MW were damaged in June 2023 [80]. Altogether, in 2024 alone, 664 MW hydropower capacity from 16 hydropower projects were damaged by flooding and landslides [81], with an approximate NPR 5 billion (approx. USD 3.7 million) loss to the power sector due to flooding and landslides [82]. A recent study has suggested that probability analysis is essential for long-term slope stability [83].

AI and machine learning techniques are increasingly being used for application in environment monitoring, data collection, and analysis of land surface characters using satellite imagery [28,84–86]. AI can be deployed to remotely sensed data for the monitoring, analysis, and decision making to develop sustainable dam areas. This can involve applying a remote sensing technique for baseline mapping of upstream and downstream parts of the dam area for forecasting hazards using training data (multiple hazards, geology, slop analysis) from previous instances and/or alternative sites. Artificial Neural Networks (ANNs) and the K-Nearest Neighbor (K-NN) model can be considered for the evaluation of the land system of complex topography elsewhere in the future [87].

We acknowledge this study is based on remote sensing data, primarily using a third-party supplier. This study specifically focuses on the dam environment under investigation. The research and analysis conducted are limited to the specific context of the dam being studied. Nevertheless, the findings and conclusions of this study may be applicable to

other dam environments or settings. Going forward, the analysis outcomes of this work, specifically the satellite-based analysis, will be developed to explore its implementation for safeguarding future damages to dam environments of more recently built storage-type hydropower projects. Further, the uncertainty in landslide dam erodibility parameters has not been taken into account in this study. This warrants further research to quantify the uncertainty associated with landslide dam material properties and sedimentation using AI technology. By addressing this uncertainty, a more comprehensive understanding of the factors influencing landslide dam behavior can be achieved. This will contribute to improved assessments and management strategies for landslide-prone areas. Modern techniques should be adopted for controlling the risk assessment and developing the information to support decisions for sustainable dam management and construction.

5. Conclusions and Further Research

This study provided an analysis framework for the monitoring and management of long-term dam environment health using satellite imagery and field-level observation, associated mainly with the reduction in the storage capacity of the reservoir from natural and anthropogenic activities. The key parameters studied included changes in surface water level, land cover, landslide impact of the dam area, mainly sedimentation deposition factors, climate change impact, and the impact of infrastructure development around the reservoir. This study highlighted the importance of monitoring and managing sedimentation in order to maintain the functionality and efficiency of the reservoir. This was applied to the evaluation of the changes to the storage capacity of the Kulekhani reservoir in Nepal from 1988 to 2020.

The surface water level in the Kulekhani dam is found to have drastically increased between 1988 and 2020, represented by the NDWI analysis using Landsat images of 0.182 and 0.405, respectively. A local site observation inferred that there is no adequate control mechanism in place to avoid the direct release and deposition of the materials released during road construction in the reservoir, typically during monsoon (high rain) incidents. We conclude that sedimentation deposition due to landslides, gully erosion, decreasing trend of rainfall, drought, and road construction activities are the major threats to the sustainable production of hydropower from the Kulekhani reservoir.

This study has mainly focused on evaluating the long-term historical trends of the dam environment. In the next step, more research is needed to evaluate the combined role of satellite imagery and advanced AI to provide a dynamic long-term production capacity and impact assessment of existing reservoirs for future climate-induced hazards. This should address the need for timely database updates and advanced machine learning algorithms customized to the problems. Further research is also warranted to assess the potential benefits of implementing an adequate sedimentation control mechanism, so that the reservoir's capacity can be preserved, enhancing its overall functionality and efficiency.

**Appendix A. Applied Landslide Risk Mapping Methodology**
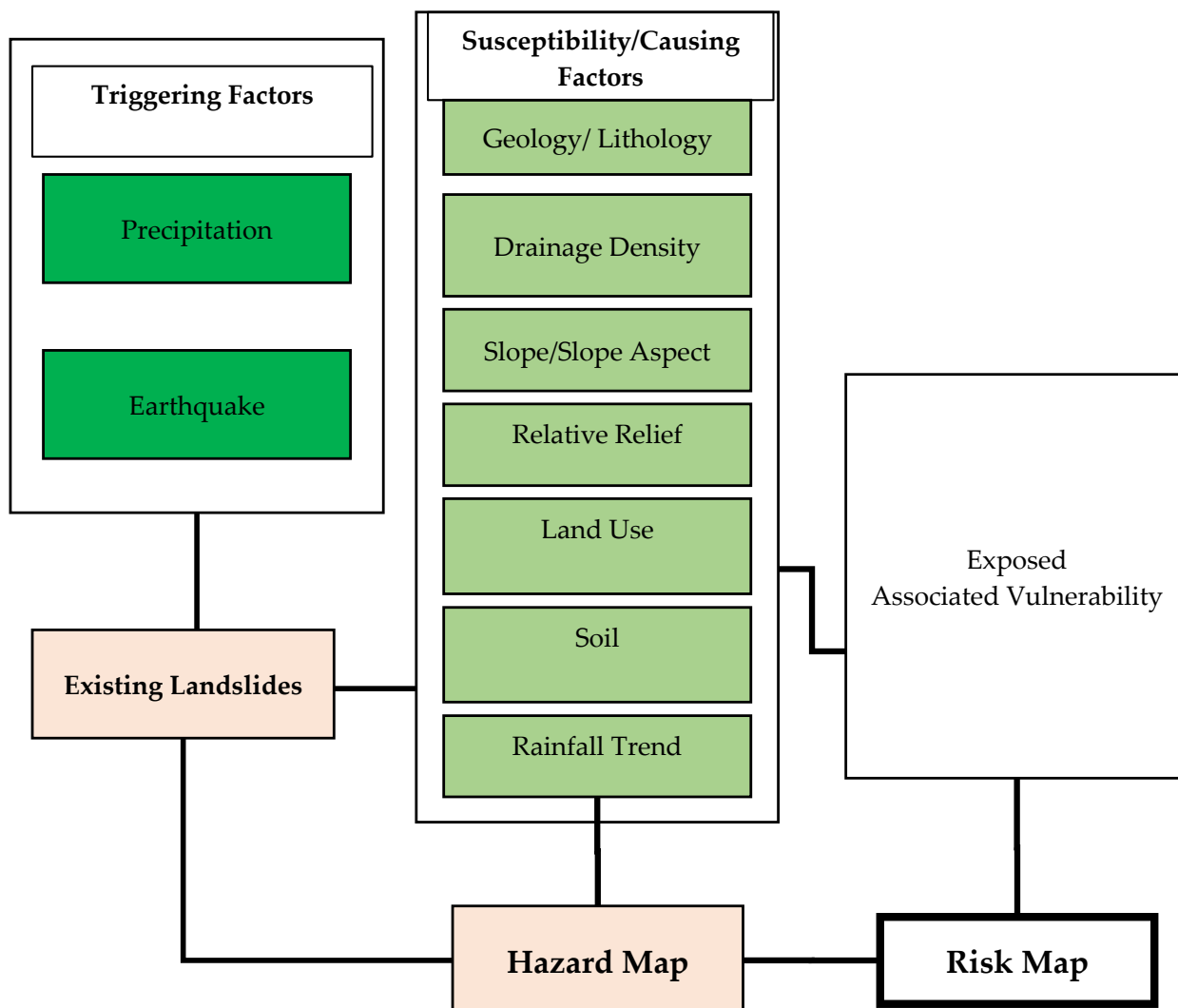
List of available data for landslide mapping.

1. Land use/land cover data using SPOT Image 2020.
2. Slope and slope aspect from SRTM DEM.
3. Relative relief derived from DEM.
4. River network from land use/land cover data, 2020, and topographical data prepared by the Survey Department of Nepal, 1996.
5. Geology data from ICIMOD.
6. Soil and Terrain (SOTER), 2009, data from SRIC Report 2009/01: Soil and Terrain database for Nepal.
7. Rainfall data from DHM, 2020, and CBS, 2008, 2013, and 2019, from 1985 to 2020.

Appendix B. Drainage, Elevation, Slope, Soil, Geology, and Seismic Risk Level Map for Landslide Evaluation
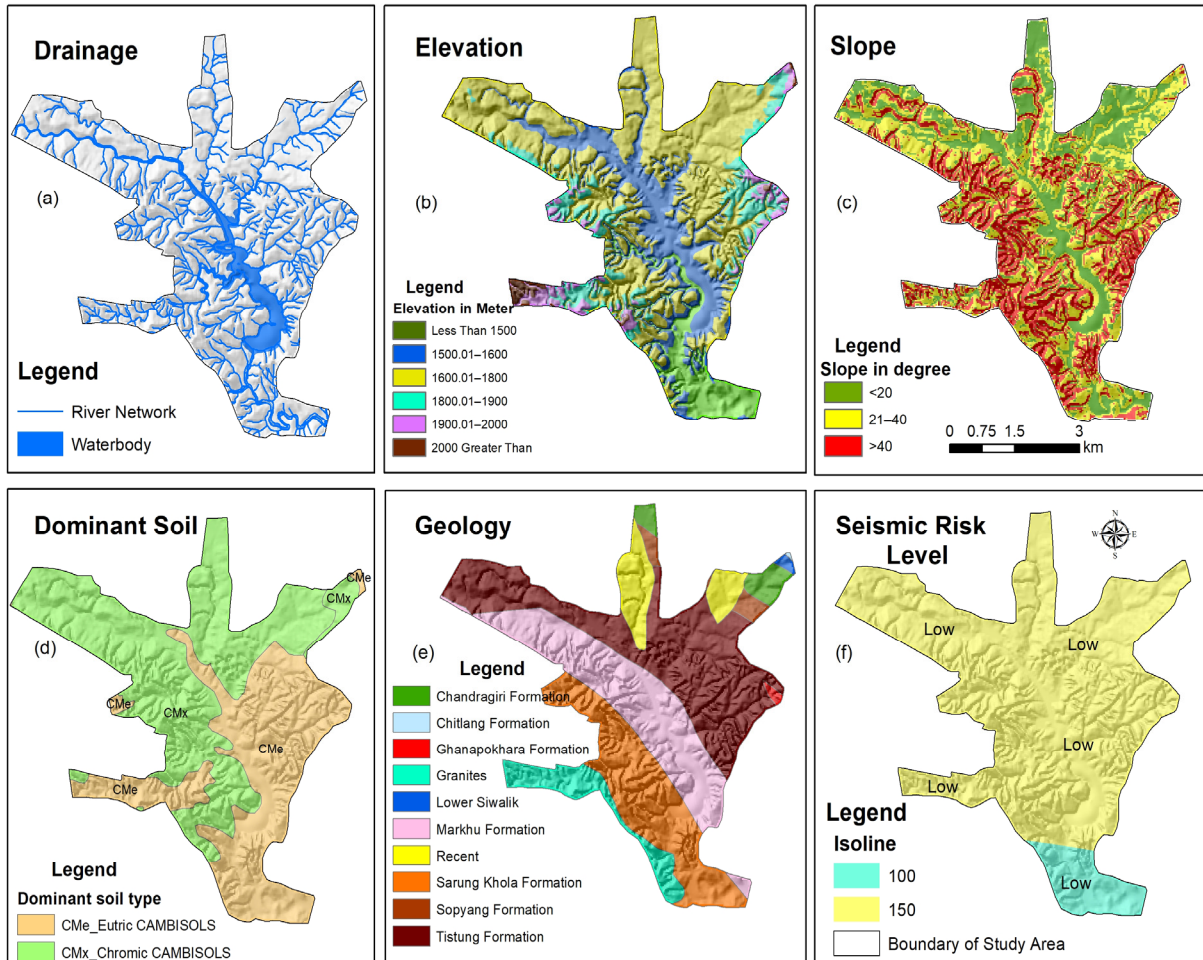
Appendix C. Trend of Land Use/Land Cover from 2004 to 2020 in the Study Area

Land Cover Change
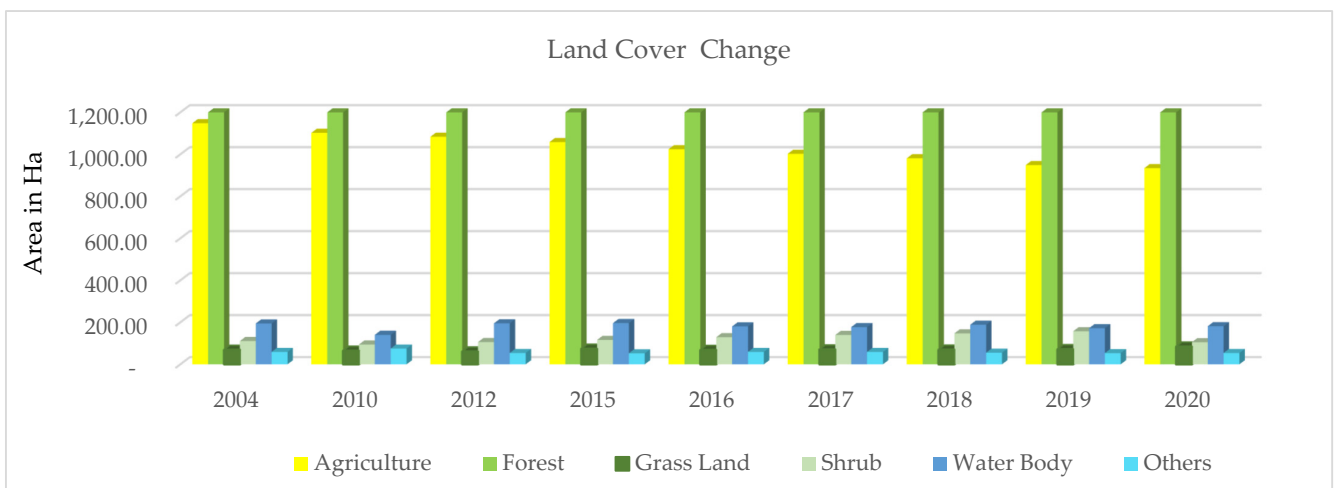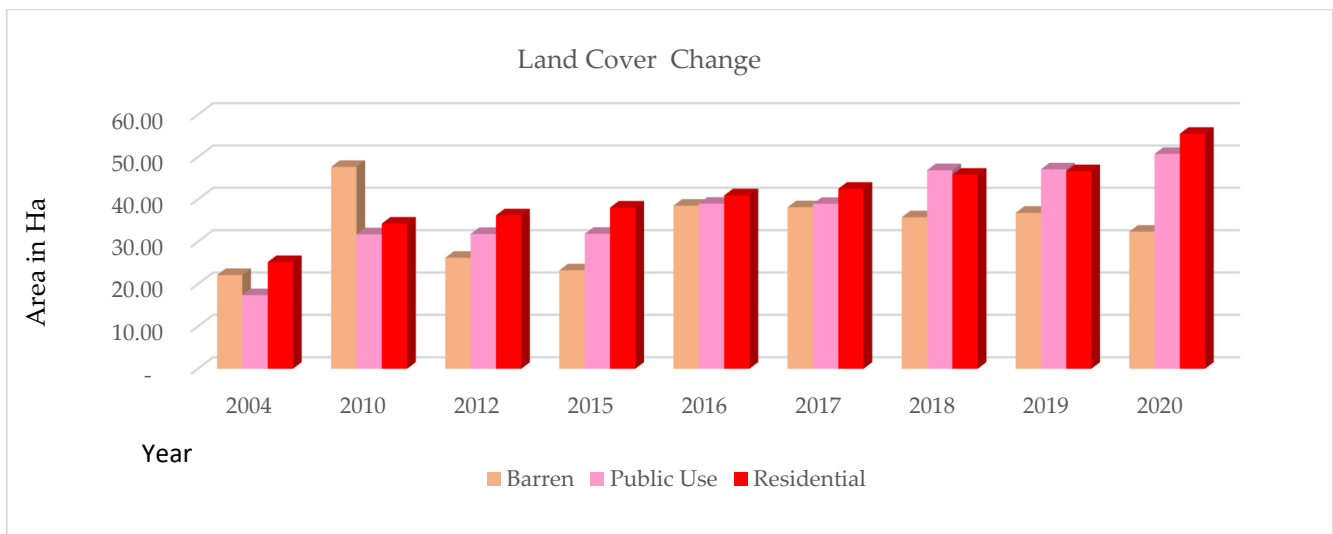
References

1. Bell, R.; Fort, M.; Götz, J.; Bernsteiner, H.; Andermann, C.; Etzlstorfer, J.; Posch, E.; Gurung, N.; Gurung, S. Major geomorphic events and natural hazards during monsoonal precipitation 2018 in the Kali Gandaki Valley, Nepal Himalaya. *Geomorphology* **2021**, *372*, 107451. [CrossRef]
2. Barros, A.; Chiao, S.; Lang, T.; Burbank, D.; Putkonen, J. *From Weather to Climate-Seasonal and Interannual Variability of Storms and Implications for Erosion Processes in the Himalaya*; Geological Society of America: Boulder, CO, USA, 2006; Volume 398, pp. 17–38.
3. Qiu, J. Killer landslides: The lasting legacy of Nepal's quake. *Nature* **2016**, *532*, 428–431. [CrossRef] [PubMed]
4. Pehlivan, M.; Madugo, C.M.; Macdonald, A.; Rayamajhi, D.; Hashash, Y.M.A.; Tiwari, B. Hydropower Infrastructure Performance after the 2015 Gorkha, Nepal, Earthquake Sequence. *Earthq. Spectra* **2017**, *33*, 115–132. [CrossRef]
5. Bhatt, R.P. Hydropower Development in Nepal—Climate Change, Impacts and Implications. *Renew. Hydropower Technol.* **2017**, *1*, 75–98. [CrossRef]
6. Ghimire, H.R.; Phuyal, S.; Singh, N.R. Environmental compliance of hydropower projects in Nepal. *Environ. Chall.* **2021**, *5*, 100307. [CrossRef]
7. Alley, K.D.; Hile, R.; Mitra, C. Visualizing Hydropower Across the Himalayas: Mapping in a time of Regulatory Decline. *Himalaya* **2014**, *34*, 9.
8. Shrestha, S.; Khatiwada, M.; Babel, M.S.; Parajuli, K. Impact of Climate Change on River Flow and Hydropower Production in Kulekhani Hydropower Project of Nepal. *Environ. Process.* **2014**, *1*, 231–250. [CrossRef]
9. Grumbine, R.E.; Pandit, M.K. Threats from India's Himalaya Dams. *Science* **2013**, *339*, 36–37. [CrossRef]
10. Sidle, R.C.; Jarihani, B.; Kaka, S.I.; Koci, J.; Al-Shaibani, A. Hydrogeomorphic processes affecting dryland gully erosion: Implications for modelling. *Prog. Phys. Geogr. Earth Environ.* **2018**, *43*, 46–64. [CrossRef]
11. Woldemichael, A.T.; Hossain, F.; Pielke, R., Sr.; Beltrán-Przekurat, A. Understanding the impact of dam-triggered land use/land cover change on the modification of extreme precipitation. *Water Resour. Res.* **2012**, *48*, 1–16. [CrossRef]
12. Hossain, F.; Degu, A.M.; Yigzaw, W.; Burian, S.; Niyogi, D.; Shepherd, J.M.; Pielke, R. Climate Feedback–Based Provisions for Dam Design, Operations, and Water Management in the 21st Century. *J. Hydrol. Eng.* **2012**, *17*, 837–850. [CrossRef]
13. Fox, G.A.; Sheshukov, A.; Cruse, R.; Kolar, R.L.; Guertault, L.; Gesch, K.R.; Dutnell, R.C. Reservoir Sedimentation and Upstream Sediment Sources: Perspectives and Future Research Needs on Streambank and Gully Erosion. *Environ. Manag.* **2016**, *57*, 945–955. [CrossRef] [PubMed]
14. Kou, P.; Xu, Q.; Jin, Z.; Tao, Y.; Yunus, A.P.; Feng, J.; Pu, C.; Yuan, S.; Xia, Y. Analyzing gully erosion and deposition patterns in loess tableland: Insights from small baseline subset interferometric synthetic aperture radar (SBAS InSAR). *Sci. Total Environ.* **2024**, *916*, 169873. [CrossRef] [PubMed]
15. Wu, S.; Hu, X.; Zheng, W.; He, C.; Zhang, G.; Zhang, H.; Wang, X. Effects of reservoir water level fluctuations and rainfall on a landslide by two-way ANOVA and K-means clustering. *Bull. Eng. Geol. Environ.* **2021**, *80*, 5405–5421. [CrossRef]
16. Lehner, B.; Beames, P.; Mulligan, M.; Zarfl, C.; De Felice, L.; van Soesbergen, A.; Thieme, M.; Garcia de Leaniz, C.; Anand, M.; Belletti, B.; et al. The Global Dam Watch database of river barrier and reservoir information for large-scale applications. *Sci. Data* **2024**, *11*, 1069. [CrossRef]
17. Tian, D.; Zhao, X.; Gao, L.; Liang, Z.; Yang, Z.; Zhang, P.; Wu, Q.; Ren, K.; Li, R.; Yang, C.; et al. Estimation of water quality variables based on machine learning model and cluster analysis-based empirical model using multi-source remote sensing data in inland reservoirs, South China. *Environ. Pollut.* **2024**, *342*, 123104. [CrossRef]
18. Dini, B.; Manconi, A.; Loew, S.; Chophel, J. The Punatsangchhu-I dam landslide illuminated by InSAR multitemporal analyses. *Sci. Rep.* **2020**, *10*, 8304. [CrossRef]

19. Iradukunda, P.; Bwambale, E. Reservoir sedimentation and its effect on storage capacity—A case study of Murera reservoir, Kenya. *Cogent Eng.* **2021**, *8*, 1917329. [CrossRef]

20. Kothyari, U. Sediment problems and sediment management in the Indian Sub-Himalayan region. In Proceedings of the Sediment Problems and Sediment Management in Asian River Basins, Hyderabad, India, 7–11 September 2009.

21. Yasarer, L.M.W.; Sturm, B.S.M. Potential impacts of climate change on reservoir services and management approaches. *Lake Reserv. Manag.* **2015**, *32*, 13–26. [CrossRef]

22. Mishra, S.K.; Veselka, T.D.; Prusevich, A.A.; Grogan, D.S.; Lammers, R.B.; Rounce, D.R.; Ali, S.H.; Christian, M.H. Differential Impact of Climate Change on the Hydropower Economics of Two River Basins in High Mountain Asia. *Front. Environ. Sci.* **2020**, *8*, 26. [CrossRef]

23. Shrestha, A.; Shrestha, S.; Tingsanchali, T.; Budhathoki, A.; Ninsawat, S. Adapting hydropower production to climate change: A case study of Kulekhani Hydropower Project in Nepal. *J. Clean. Prod.* **2021**, *279*, 123483. [CrossRef]

24. Hwang, J.; Lall, U. Increasing dam failure risk in the USA due to compound rainfall clusters as climate changes. *Npj Nat. Hazards* **2024**, *1*, 27. [CrossRef]

25. Ahmad, M.-u.-D.; Peña-Arancibia, J.L.; Yu, Y.; Stewart, J.P.; Podger, G.M.; Kirby, J.M. Climate change and reservoir sedimentation implications for irrigated agriculture in the Indus Basin Irrigation System in Pakistan. *J. Hydrol.* **2021**, *603*, 126967. [CrossRef]

26. Lempérière, F. Dams and Floods. *Engineering* **2017**, *3*, 144–149. [CrossRef]

27. Zhang, T.; Wang, W.; An, B. A massive lateral moraine collapse triggered the 2023 South Lhonak Lake outburst flood, Sikkim Himalayas. *Landslides* **2024**, 1–13. [CrossRef]

28. Himeur, Y.; Rimal, B.; Tiwary, A.; Amira, A. Using artificial intelligence and data fusion for environmental monitoring: A review and future perspectives. *Inf. Fusion* **2022**, *86–87*, 44–75. [CrossRef]

29. Krzton, W.; Walusiak, E.; Wilk-Wozniak, E. Possible consequences of climate change on global water resources stored in dam reservoirs. *Sci. Total Environ.* **2022**, *830*, 154646. [CrossRef]

30. Mackey, B.H.; Roering, J.J.; Lamb, M.P. Landslide-dammed paleolake perturbs marine sedimentation and drives genetic change in anadromous fish. *Proc. Natl. Acad. Sci. USA* **2011**, *108*, 18905. [CrossRef]

31. Petley, D.N.; Hearn, G.J.; Hart, A.B.; Rosser, N.J.; Dunning, S.A.; Oven, K.J.; Mitchell, W.A. Trends in landslide occurrence in Nepal. *Nat. Hazards* **2007**, *43*, 23–44. [CrossRef]

32. McAdoo, B.G.; Quak, M.; Gnyawali, K.R.; Adhikari, B.R.; Devkota, S.; Rajbhandari, P.L.; Sudmeier-Rieux, K. Roads and landslides in Nepal: How development affects environmental risk. *Nat. Hazards Earth Syst. Sci.* **2018**, *18*, 3203–3210. [CrossRef]

33. Choudhary, S.S.; Ghosh, S.K. Surface Water Area Extraction by Using Water Indices and DFPS Method Applied to Satellites Data. *Sens. Imaging* **2022**, *23*, 33. [CrossRef]

34. Zhang, M.; Wang, X.; Shi, C.; Yan, D. Automated Glacier Extraction Index by Optimization of Red/SWIR and NIR /SWIR Ratio Index for Glacier Mapping Using Landsat Imagery. *Water* **2019**, *11*, 1223. [CrossRef]

35. Feyisa, G.L.; Meilby, H.; Fensholt, R.; Proud, S.R. Automated Water Extraction Index: A new technique for surface water mapping using Landsat imagery. *Remote Sens. Environ.* **2014**, *140*, 23–35. [CrossRef]

36. McFeeters, S.K. The use of the Normalized Difference Water Index (NDWI) in the delineation of open water features. *Int. J. Remote Sens.* **1996**, *17*, 1425–1432. [CrossRef]

37. Ji, L.; Zhang, L.; Wylie, B.K. Analysis of dynamic thresholds for the normalized difference water index. *Photogramm. Eng. Remote Sens.* **2009**, *75*, 1307–1317. [CrossRef]

38. Li, D.; Shangguan, D.; Anjum, M.N. Glacial Lake Inventory Derived from Landsat 8 OLI in 2016–2018 in China–Pakistan Economic Corridor. *ISPRS Int. J. Geo-Inf.* **2020**, *9*, 294. [CrossRef]

39. Xu, H. Modification of normalised difference water index (NDWI) to enhance open water features in remotely sensed imagery. *Int. J. Remote Sens.* **2006**, *27*, 3025–3033. [CrossRef]

40. Lacaux, J.P.; Tourre, Y.M.; Vignolles, C.; Ndione, J.A.; Lafaye, M. Classification of ponds from high-spatial resolution remote sensing: Application to Rift Valley Fever epidemics in Senegal. *Remote Sens. Environ.* **2007**, *106*, 66–74. [CrossRef]

41. Hall, D.K.; Riggs, G.A.; Salomonson, V.V. Development of methods for mapping global snow cover using moderate resolution imaging spectroradiometer data. *Remote Sens. Environ.* **1995**, *54*, 127–140. [CrossRef]

42. Donmez, C.; Berberoglu, S.; Cicekli, S.Y.; Cilek, A.; Arslan, A.N. Mapping snow cover using landsat data: Toward a fine-resolution water-resistant snow index. *Meteorol. Atmos. Phys.* **2020**, *133*, 281–294. [CrossRef]

43. Xiong, L.; Deng, R.; Li, J.; Liu, X.; Qin, Y.; Liang, Y.; Liu, Y. Subpixel Surface Water Extraction (SSWE) Using Landsat 8 OLI Data. *Water* **2018**, *10*, 653. [CrossRef]

44. Schulz, D.; Yin, H.; Tischbein, B.; Verleysdonk, S.; Adamou, R.; Kumar, N. Land use mapping using Sentinel-1 and Sentinel-2 time series in a heterogeneous landscape in Niger, Sahel. *ISPRS J. Photogramm. Remote Sens.* **2021**, *178*, 97–111. [CrossRef]

45. Elmahdy, S.I.; Mohamed, M.M. The impact of land use land cover on groundwater level and quality in the Emirate of Abu Dhabi, UAE: An integration approach using remote sensing and hydrological data. *Geocarto Int.* **2023**, *38*, 2272664. [CrossRef]

46. Fallah Shamsi, S.R.; Zakeri-Anaraki, S.; Masoudi, M. Chapter 41—Kernel-based granulometry of textural pattern measures on satellite imageries for fine-grain sparse woodlands mapping. In *Computers in Earth and Environmental Sciences*; Pourghasemi, H.R., Ed.; Elsevier: Amsterdam, The Netherlands, 2022; pp. 563–576.

47. Devkota, P.; Dhakal, S.; Shrestha, S.; Shrestha, U.B. Land use land cover changes in the major cities of Nepal from 1990 to 2020. *Environ. Sustain. Indic.* **2023**, *17*, 100227. [CrossRef]

48. Li, M.; Wu, P.; Wang, B.; Park, H.; Yang, H.; Wu, Y. A Deep Learning Method of Water Body Extraction From High Resolution Remote Sensing Images With Multisensors. *IEEE J. Sel. Top. Appl. Earth Obs. Remote Sens.* **2021**, *14*, 3120–3132. [CrossRef]

49. *NEF: Siltation in Kulekhani Reservoir Affects Power*; Nepal Energy Forum: Hetaunda, Nepal, 14 February 2013. Available online: http://www.nepalenergyforum.com/siltation-in-kulekhani-reservoir-affects-power/ (accessed on 16 August 2024).

50. Ghimire, S.; Dhungana, N.; Upadhaya, S. Impacts of Climate Change on Water Availability and Reservoir Based Hydropower. *J. For. Nat. Resour. Manag.* **2019**, *1*, 52–68. [CrossRef]

51. Dhital, M.; Manandhar, S.; Hino, T.; Daisuke, S. Sediment accumulation in the Kulekhani reservoir due to the 1993 debris flows and landslides. In Proceedings of the 9th International Symposium on Lowland Technology (ISLT 2014), Saga, Japan, 22–26 June 2014.

52. Pandey, M.R.; Chitrakara, G.R.; Kafle, B.; Sapkota, S.N.; Rajaure, S.; Gautam, U.P. *Seismic Hazard Map of Nepal*; National Seismological Centre: Kathmandu, Nepal, 2002.

53. GoN. Topographical Map. In *Government of Nepal MoLRaM*; Survey Department, Topographic Survey Branch, Ed.; Min Bhawan: Kathmandu, Nepal, 1996.

54. Silva, L.P.e.; Xavier, A.P.C.; da Silva, R.M.; Santos, C.A.G. Modeling land cover change based on an artificial neural network for a semiarid river basin in northeastern Brazil. *Glob. Ecol. Conserv.* **2020**, *21*, e00811. [CrossRef]

55. Aguilera, M.A.Z. Classification of Land-Cover Through Machine Learning Algorithms for Fusion of Sentinel-2a and Planetscope Imagery. In Proceedings of the 2020 IEEE Latin American GRSS & ISPRS Remote Sensing Conference (LAGIRS), Santiago, Chile, 22–26 March 2020. Int. Arch. Photogramm. Remote Sens. Spatial Inf. Sci., XLII-3/W12-2020, 361–368. [CrossRef]

56. Estacio, I.; Sianipar, C.P.M.; Onitsuka, K.; Basu, M.; Hoshino, S. A statistical model of land use/cover change integrating logistic and linear models: An application to agricultural abandonment. *Int. J. Appl. Earth Obs. Geoinf.* **2023**, *120*, 103339. [CrossRef]

57. Tikuye, B.G.; Rusnak, M.; Manjunatha, B.R.; Jose, J. Land Use and Land Cover Change Detection Using the Random Forest Approach: The Case of The Upper Blue Nile River Basin, Ethiopia. *Glob. Chall.* **2023**, *7*, 2300155. [CrossRef]

58. Rimal, B.; Rijal, S.; Stork, N.; Keshtkar, H.; Zhang, L. Forest restoration and support for sustainable ecosystems in the Gandaki Basin, Nepal. *Environ. Monit. Assess.* **2021**, *193*, 563. [CrossRef]

59. Jamsran, B.-E.; Lin, C.; Byambakhuu, I.; Raash, J.; Akhmadi, K. Applying a support vector model to assess land cover changes in the Uvs Lake Basin ecoregion in Mongolia. *Inf. Process. Agric.* **2019**, *6*, 158–169. [CrossRef]

60. Ibrahim Mahmoud, M.; Duker, A.; Conrad, C.; Thiel, M.; Shaba Ahmad, H. Analysis of Settlement Expansion and Urban Growth Modelling Using Geoinformation for Assessing Potential Impacts of Urbanization on Climate in Abuja City, Nigeria. *Remote Sens.* **2016**, *8*, 220. [CrossRef]

61. Huang, C.; Davis, L.S.; Townshend, J.R.G. An assessment of support vector machines for land cover classification. *Int. J. Remote Sens.* **2002**, *23*, 725–749. [CrossRef]

62. Mubea, K.; Menz, G. Monitoring Land-Use Change in Nakuru (Kenya) Using Multi-Sensor Satellite Data. *Adv. Remote Sens.* **2012**, *1*, 74–84. [CrossRef]

63. Pal, M.; Mather, P.M. Support vector machines for classification in remote sensing. *Int. J. Remote Sens.* **2005**, *26*, 1007–1011. [CrossRef]

64. Sothe, C.; Almeida, C.; Liesenberg, V.; Schimalski, M. Evaluating Sentinel-2 and Landsat-8 Data to Map Sucessional Forest Stages in a Subtropical Forest in Southern Brazil. *Remote Sens.* **2017**, *9*, 838. [CrossRef]

65. Xiong, J.; Thenkabail, P.; Tilton, J.; Gumma, M.; Teluguntla, P.; Oliphant, A.; Congalton, R.; Yadav, K.; Gorelick, N. Nominal 30-m Cropland Extent Map of Continental Africa by Integrating Pixel-Based and Object-Based Algorithms Using Sentinel-2 and Landsat-8 Data on Google Earth Engine. *Remote Sens.* **2017**, *9*, 1065. [CrossRef]

66. Zhao, H.; Chen, F.; Zhang, M. A Systematic Extraction Approach for Mapping Glacial Lakes in High Mountain Regions of Asia. *IEEE J. Sel. Top. Appl. Earth Obs. Remote Sens.* **2018**, *11*, 2788–2799. [CrossRef]

67. Acharya, T.D.; Subedi, A.; Lee, D.H. Evaluation of Machine Learning Algorithms for Surface Water Extraction in a Landsat 8 Scene of Nepal. *Sensors* **2019**, *19*, 2769. [CrossRef]

68. Yan, D.; Huang, C.; Ma, N.; Zhang, Y. Improved Landsat-Based Water and Snow Indices for Extracting Lake and Snow Cover/Glacier in the Tibetan Plateau. *Water* **2020**, *12*, 1339. [CrossRef]

69. Chicas, S.D.; Li, H.; Mizoue, N.; Ota, T.; Du, Y.; Somogyvári, M. Landslide susceptibility mapping core-base factors and models' performance variability: A systematic review. *Nat. Hazards* **2024**, *2024*, 1–21. [CrossRef]

70. Gaidzik, K.; Ramírez-Herrera, M.T. The importance of input data on landslide susceptibility mapping. *Sci. Rep.* **2021**, *11*, 19334. [CrossRef] [PubMed]

71. Hossain, M.D.T.; Chackroborty, R.D.; Intisar, L.; Al Toufiq Shuvo, S.; Al Rakib, A.; Kafy, A.-A. Landslide Susceptibility and Risk Assessment in Hilly Regions of Bangladesh: A Geostatistical and Geospatial Modeling Approach for Sustainability. In *Landslide: Susceptibility, Risk Assessment and Sustainability: Application of Geostatistical and Geospatial Modeling*; Panda, G.K., Shaw, R., Eds.; Springer Nature: Cham, Switzerland, 2024.

72. Quaicoe, J. Landslide Risk and Vulnerability; Real Issues, Thoughts and Perspectives. In *Landslide: Susceptibility, Risk Assessment and Sustainability: Application of Geostatistical and Geospatial Modeling*; Panda, G.K., Shaw, R., Pal, S.C., Chatterjee, U., Saha, A., Eds.; Springer Nature: Cham, Switzerland, 2024; pp. 3–23.

73. Youssef, K.; Shao, K.; Moon, S.; Bouchard, L.S. Landslide susceptibility modeling by interpretable neural network. *Commun. Earth Environ.* **2023**, *4*, 162. [CrossRef]

74. Jaafari, A. An Overview of Triggering and Causing Factors of Landslides. In *Landslides in the Himalayan Region: Risk Assessment and Mitigation Strategy for Sustainable Management*; Chatterjee, U., Lalmalsawmzauva, K.C., Biswas, B., Pal, S.C., Eds.; Springer Nature: Singapore, 2024; pp. 25–45.

75. Shrestha, A.; Ghimire, S.; Pokharel, A.; Dhami, S.; Karki, S.; Awasthi, B.; Acharya, T. Landslide Susceptibility Mapping in Budhi Gandaki River Sub-Basin Using Frequency Ratio and Statistical Information Index. *Bull. Nepal Hydrogeol. Assoc.* **2021**, *6*, 97–120.

76. Muñoz-Torrero Manchado, A.; Allen, S.K.; Ballesteros-Cánovas, J.A.; Dhakal, A.; Dhital, M.R.; Stoffel, M. Three decades of landslide activity in western Nepal: New insights into trends and climate drivers. *Landslides* **2021**, *18*, 2001–2015. [CrossRef]

77. Dhakal, M. Climate Change Impact on Reservoir Based Hydropower Generation in Nepal: A Case Study of Kulekhani Hydropower Plant. Master's Thesis, Pokhara University, Pokhara, Nepal, 2011.

78. Ngondo, J.; Mango, J.; Nobert, J.; Dubi, A.; Li, X.; Cheng, H. Hydrological Response of the Wami–Ruvu Basin to Land-Use and Land-Cover Changes and Its Impacts for the Future. *Water* **2022**, *14*, 184. [CrossRef]

79. Republica, Water Level at Kulekhani I Hydropower Station Recedes, Operating at Full Capacity, Republica. 28 September 2024. Available online: https://myrepublica.nagariknetwork.com/news/water-level-at-kulekhani-i-hydropower-station-recedes-operating-at-full-capacity/?categoryId=81 (accessed on 16 October 2024).

80. Lamsal, H. Lack of Disaster Preparedness Causing Severe Damages to Hydropower Projects in Nepal, Myrepublica. 27 January 2024. Available online: https://myrepublica.nagariknetwork.com/news/lack-of-flood-preparedness-inflicts-severe-damage-on-hydropower-projects/ (accessed on 16 August 2024).

81. Prasain, S. Heavy Rains Inflict an Estimated Rs17 Billion Loss on Nepal. Kathmandu Post. 14 October 2024. Available online: https://kathmandupost.com/national/2024/10/01/heavy-rains-inflict-rs17-billion-loss-on-nepal (accessed on 16 October 2024).

82. Nepal, F. Nepal's Power Sector Faces Billions in Losses for Second Year Due to Floods and Landslides, Fiscal Nepal. 14 October 2024. Available online: https://www.fiscalnepal.com/2024/09/30/18165/nepals-power-sector-faces-billions-in-losses-for-second-year-due-to-floods-and-landslides/#ixzz8odc1kM33 (accessed on 16 October 2024).

83. Regmi, S.; Dahal, R.K. Consequences of slope instability and existing practices of mitigation in hydropower projects of Nepal. *Geoenviron. Disasters* **2024**, *11*, 26. [CrossRef]

84. He, J.; Zhang, L.; Xiao, T.; Chen, C. Emergency risk management for landslide dam breaks in 2018 on the Yangtze River, China. *Resilient Cities Struct.* **2022**, *1*, 1–11. [CrossRef]

85. Suo, L.; Niu, X.; Xie, H. 6.07—The Three Gorges Project in China. In *Comprehensive Renewable Energy*; Sayigh, A., Ed.; Elsevier: Oxford, UK, 2012; pp. 179–226.

86. Abdi, A.M. Land cover and land use classification performance of machine learning algorithms in a boreal landscape using Sentinel-2 data. *GISci. Remote Sens.* **2020**, *57*, 1–20. [CrossRef]

87. Maxwell, A.E.; Warner, T.A.; Fang, F. Implementation of machine-learning classification in remote sensing: An applied review. *Int. J. Remote Sens.* **2018**, *39*, 2784–2817. [CrossRef]